HHS Public Access

Author manuscript

Nature. Author manuscript; available in PMC 2024 May 01.

Published in final edited form as:

Nature. 2023 May ; 617(7959): 154–161. doi:10.1038/s41586-023-05943-7.

Alternative Cdc20 translational isoforms tune mitotic arrest duration

Mary-Jane Tsang[1,2], **Iain M. Cheeseman**[1,2,*]

[1]Whitehead Institute for Biomedical Research, 455 Main Street, Cambridge, MA 02142

[2]Department of Biology, Massachusetts Institute of Technology, Cambridge, MA 02142

Summary

Mitotic defects activate the Spindle Assembly Checkpoint (SAC), which inhibits the APC/C co-activator Cdc20 to induce a prolonged cell cycle arrest [1,2]. Once errors are corrected, the SAC is silenced allowing anaphase onset to occur. However, in the presence of persistent, unresolvable errors, cells can undergo “mitotic slippage”, exiting mitosis into a tetraploid G1 state and escaping the cell death that results from a prolonged arrest. The molecular logic that allows cells to balance these dueling mitotic arrest and slippage behaviors remains unclear. Here we demonstrate that human cells modulate their mitotic arrest duration through the presence of conserved, alternative Cdc20 translational isoforms. Downstream translation initiation results in a truncated Cdc20 isoform that is resistant to SAC-mediated inhibition and promotes mitotic exit even in the presence of mitotic perturbations. Our work supports a model in which the relative levels of Cdc20 translational isoforms control mitotic arrest duration. During a prolonged mitotic arrest, new protein synthesis and differential Cdc20 isoform turnover create a timer, with mitotic exit occurring once the truncated M43 isoform achieves sufficient levels. Targeted molecular changes or naturally-occurring cancer mutations that alter Cdc20 isoform ratios or its translational control modulate mitotic arrest duration and anti-mitotic drug sensitivity, with potential implications for the diagnosis and treatment of human cancers.

Alternative Cdc20 proteoforms

Cdc20 is a critical co-activator of the anaphase-promoting complex, also known as the cyclosome (APC/C), an E3 ubiquitin ligase that directs the ubiquitination and degradation of mitotic substrates to promote chromosome segregation and mitotic exit [3] (Fig. 1A). Consistent with prior reports [4-6], we observed a clear mitotic arrest in human HeLa cells following treatment with Cdc20 siRNAs or using an inducible CRISPR/Cas9 gene-targeting strategy [7] with an sgRNA recognizing a region within exon 3 (sgExon3) (Fig. 1B). In contrast, Cas9-mediated DNA cleavage with guides targeting *CDC20* near the start codon

*Correspondence and requests for materials should be addressed to Iain Cheeseman (icheese@wi.mit.edu). Phone: (617) 324-2503.

Author Contributions

Conceptualization – MJT, IMC; Methodology – MJT; Validation – MJT; Investigation – MJT; Writing - Original Draft Preparation – MJT, IMC; Writing – Review & Editing – MJT, IMC; Visualization – MJT; Supervision: IMC; Funding Acquisition: IMC, MJT

Competing Interest Statement

A patent has been filed on all aspects of this work by Whitehead Institute. Inventors: Iain Cheeseman and Mary-Jane Tsang; Application #: WIBR-178-001; IC18-02. The patent and initial disclosure have been filed, but the consideration is still pending.

(sgM1) or within exon 1 (sgExon1) did not cause a potent mitotic arrest (Fig. 1B). Cdc20 does not display alternative mRNA splicing within its coding sequence [8], and thus prior work has assumed that Cdc20 exists as a single ~55 kDa protein. However, Western blots using antibodies recognizing the Cdc20 C-terminus (aa 450-499) additionally detected two lower molecular-weight species (Fig. 1C). These protein bands were not due to phosphorylation (Extended Fig. 1A) and were eliminated by siRNA treatment targeting the Cdc20 mRNA (Fig. 1C). Similar lower molecular-weight Cdc20 species were also detected in multiple human cancer cell lines (A549, DLD-1, and U2OS), the non-transformed human hTERT RPE-1 cell line, and the mouse NIH/3T3 cell line (Extended Fig. 1B).

Although Cdc20 is essential for viability [5,9,10], we were able to isolate stable clonal HeLa cell lines lacking the canonical full-length Cdc20 protein (Fig. 1C) by eliminating the M1 ATG start codon (ΔM1; see Extended Fig. 1C) or creating frame-shift insertions that result in premature stop codons for both *CDC20* alleles (M1-stop; see Extended Fig. 1D). For these ΔM1 and M1-stop mutants, the lower molecular-weight protein bands were now the major Cdc20 species and were eliminated by Cdc20 siRNA treatment (Fig. 1C). This suggests that these proteins reflect N-terminally truncated alternative protein isoforms (proteoforms [11]). Despite the absence of full-length Cdc20, both the ΔM1 and M1-stop mutant cell lines were viable with either similar (M1-stop; Extended Fig. 1E-F) or modestly reduced growth rates and mitotic duration (ΔM1; Extended Fig. 1E-F) relative to controls. Importantly, both mutants were still dependent on Cdc20 for mitotic progression, as treatment with Cdc20 siRNAs resulted in a potent metaphase arrest (Fig. 1D). Together, these results demonstrate that human cells express multiple Cdc20 proteoforms such that the canonical full-length Cdc20 protein is not strictly essential for viability or mitotic progression.

Cdc20 alternative translation initiation

We next sought to determine the nature of the alternative Cdc20 proteoforms. Cdc20 contains potential downstream translation start sites at amino acid positions 43 and 88 that are conserved across mammals, diverse tetrapod species, and echinoderms (Fig. 1E; data not shown). Based on mass spectrometry analysis of Cdc20-mEGFP isolated from cells tagged at the C-terminus of the endogenous *CDC20* locus, we identified peptides corresponding to translation initiation at the M1, M43, and M88 start sites (Extended Fig. 2A-C). Using an RNAi-based gene-replacement strategy (Fig. 1F), we found that wild-type *CDC20* cDNA recapitulated the endogenous Cdc20 isoform pattern with the presence of three protein species, indicating that multiple Cdc20 proteoforms can be generated from a single mRNA transcript. Mutating M43 or M88 to leucine selectively eliminated the corresponding protein products demonstrating that these start codons are responsible for the truncated Cdc20 proteoforms.

Eukaryotic translation initiation is typically accomplished by a scanning mechanism in which the 40S ribosomal subunit is loaded at the 5’-cap and translocates along the mRNA until it initiates translation at the first AUG encountered [12]. Translation at downstream start codons can occur by translational re-initiation or leaky scanning in which a fraction of 40S ribosomal subunits continue beyond the first AUG to initiate at a downstream

AUG [13,14]. Consistent with leaky ribosome scanning, deletion of the *CDC20* M1 start codon in either the ΔM1 mutant cell line (Fig. 1C) or the ΔM1 ectopic construct (Fig. 1F) resulted in increased initiation at the downstream M43 and M88 start codons. Leaky ribosomal scanning occurs when the translational context of the first AUG is suboptimal [14]. Indeed, we found that RNAi-based replacements introducing a strong consensus Kozak sequence at the M1 start site ("optimal-Kozak" construct; Fig. 1E) resulted in increased levels of the full-length Cdc20 protein and a concomitant decrease in the M43 and M88 isoforms (Fig. 1G). Conversely, further weakening the translational context at the M1 start site with an "anti-Kozak" sequence reduced expression of the full-length protein while allowing increased M43 and M88 translation initiation (Fig. 1G). These results are consistent with downstream translation initiation relying on leaky ribosome scanning such that the translational context surrounding the M1 start site determines the relative expression of the truncated proteoforms.

In analyzing the *CDC20* mRNA sequence, we identified two additional out-of-frame AUG start codons between M1 and M43 (Fig. 1E), which would be predicted to capture scanning ribosomes to prevent them from reaching M43 or M88. These out-of-frame start codons are conserved across mammals and are predicted to produce a 78 amino acid alternative open reading frame (altORF) peptide with a conserved stop site present downstream of the M88 codon (Extended Fig. 2D-E). Using frame shift mutant cell lines that connect the predicted altORF sequence with downstream regions of the Cdc20 protein (Extended Fig. 3A-B), we detected chimeric altATG-Cdc20 proteins by Western blotting (Extended Fig. 3C). This indicates that the alternative out-of-frame AUGs within *CDC20* are functional for translation initiation. Using RNAi-mediated replacements, we found that eliminating the alternative start sites with silent mutations (altATGmutx2; Fig. 1E) resulted in increased M43 and M88 levels without altering full-length protein levels (Fig. 1H). Reciprocally, introducing additional out-of-frame start codon(s) before the M43 start site ("addATG") prevented translation of the M43 isoform. Overall, our work suggests that M43 and M88 proteoform expression relies on leaky ribosome scanning such that their translation is controlled by multiple sequence features within the Cdc20 mRNA.

Cdc20 M43 is active but SAC-deficient

We next sought to define the functional properties of the alternative Cdc20 proteoforms, which lack conserved N-terminal residues. Similar to full-length Cdc20, N-terminal mEGFP-Cdc20 fusions of the M43 and M88 isoforms localized to kinetochores (Fig. 2A), consistent with Cdc20 kinetochore recruitment requiring its C-terminal WD40 domains [15,16]. Based on immunoprecipitations of mEGFP-Cdc20 constructs, all three Cdc20 proteoforms were able to interact with the APC/C (APC7), the mitotic checkpoint complex (MCC; Bub3), and endogenous full-length Cdc20 (Fig. 2B). Since the inhibited APC/C-MCC complex contains two distinct Cdc20 molecules [17], our results suggest that the truncated Cdc20 proteoforms are incorporated into the APC/C-MCC complex with full-length Cdc20 present in the second APC/C-MCC binding site. In the absence of full-length Cdc20 (M1-stop mutant), the truncated Cdc20 proteoforms still interacted with the APC/C, MCC, and possibly within the APC/C-MCC complex, but with reduced binding (Extended Fig. 2F). Using a CRISPR/Cas9-mediated gene replacement strategy, full-length Cdc20 or

Cdc20 M43, but not the M88 isoform, rescued the depletion of endogenous Cdc20 and were functional for mitotic progression (Fig. 1B, 2C). The inability of the M88 isoform to promote mitotic progression is likely due to the absence of the critical “C-box” motif at residues 77-83, which is required for efficient APC/C binding and activation (Fig. 1E; [18-20]).

The Cdc20 M43 and M88 isoforms lack a conserved motif (Box1 or BM1; aa 27-34) that is required for robust Cdc20-Mad1 interactions and SAC signaling (Fig. 1E) [21-23]. Therefore, ΔM1 or M1-stop mutant cells lacking full-length Cdc20 are predicted to display an altered mitotic arrest in response to the Spindle Assembly Checkpoint. Treatment with the Eg5/Kif11-inhibitor STLC prevents bipolar spindle formation, resulting in SAC activation and an extended mitotic arrest. In time-lapse experiments, after entering mitosis, STLC-treated control HeLa cells remained arrested for the duration of our analysis (>10 h) (Fig. 2D). In contrast, ΔM1 and M1-stop mutants displayed potent SAC defects with cells exiting mitosis within a few hours despite the presence of STLC (Fig. 2D). Similar mitotic arrest defects were also observed when M1-stop cells were treated with diverse anti-mitotic drugs (Fig. 2E). This premature mitotic exit was suppressed by treatment with the APC/C-inhibitor proTAME [24] (Extended Fig. 4A), indicating that the mitotic exit in ΔM1 and M1-stop mutant cells reflects premature APC/C activation. Similarly, RNAi-based depletion of Cdh1, which acts as co-activator of the APC/C in late mitosis [25], did not alter the premature mitotic exit of ΔM1 and M1-stop mutant cells (Extended Fig. 4B) indicating that Cdh1 does not substitute for full-length Cdc20 in these cell lines. The SAC defects in these mutant cell lines are also not due to second-site mutations or long-term adaptation as Cdc20 replacements using wild-type *CDC20* cDNA restored prolonged mitotic arrest behavior to the ΔM1 and M1-stop cell lines (Extended Fig. 4C) and SAC defects were observed following acute depletion of full-length Cdc20 (Extended Fig. 4D). Finally, Bub1 and Mad2 localized to kinetochores in ΔM1 and M1-stop mutant cell lines treated with the microtubule-depolymerizing drug nocodazole similar to controls (Extended Fig. 4E), suggesting that upstream SAC activation occurs effectively [1].

Despite evidence for upstream SAC activation, both the ΔM1 and M1-stop mutant cell lines behaved functionally as if the SAC was absent (Fig. 2D). Indeed, the premature mitotic exit in STLC-treated ΔM1 mutant cells was not exacerbated further by weakening the SAC by treatment with either the Mps1 inhibitor, AZ3146 (Extended Fig. 4F, Extended Table 1), or siRNAs against Mad2 (Extended Fig. 4G, Extended Table 1). However, AZ3146 treatment or Mad2 RNAi reduced the arrest of the M1-stop mutant, resulting in a mitotic duration similar to that of the ΔM1 mutant (Extended Table 1). To determine the basis for the SAC-resistance of the truncated Cdc20 proteoforms, we used RNAi-based replacements to analyze the requirements for N-terminal Cdc20 residues. Mutating the Box 1 motif [21,22] (Box1-Ala), preventing Mad2-Cdc20 binding using a R132A mutant that abrogates MCC formation and SAC signaling [18], or eliminating CDK-mediated phosphorylation of Cdc20 that is proposed to modulate APC/C binding and activation [26-28] (Extended Fig. 5A) resulted in significant reductions in mitotic arrest duration (Extended Fig. 5B-D). However, in each case, these were less dramatic than the ΔM1 construct lacking the first 42 amino acids (Extended Fig. 5B-D). Together, our results demonstrate that the truncated Cdc20 proteoforms are not effectively inhibited by the SAC due to the absence of multiple

conserved N-terminal sequences, resulting in premature APC/C activation and mitotic slippage in the presence of anti-mitotic drugs.

Cdc20 proteoforms tune mitotic duration

Control cells co-express multiple Cdc20 translational proteoforms, including the full-length protein (Fig. 1C; Extended Fig. 1B), such that these proteoforms must compete for APC/C binding. To test whether the truncated Cdc20 proteoforms can modulate mitotic arrest timing in the presence of full-length Cdc20, we altered the relative Cdc20 proteoform levels using ectopic expression of *CDC20* cDNA constructs in HeLa cells. Overexpression of a wild-type *CDC20* construct encoding all three proteoforms resulted in increased Cdc20 levels but did not substantially alter the mitotic arrest duration in the presence of STLC (Fig. 3A). In contrast, *CDC20-ΔM1* expression to increase the truncated Cdc20 isoform levels caused a dramatic increase in mitotic slippage (Fig. 3A). Preventing the increased expression of the M43 isoform in the *CDC20-ΔM1* construct using an M43L mutation fully suppressed the induced mitotic slippage phenotype, whereas an M88L mutation had little effect (Fig. 3A). Similarly, RNAi-based replacements with the altATGmutx2 construct, which increases the truncated Cdc20 isoform levels by disrupting altORF expression (see Fig. 1H), resulted in a significant reduction in mitotic arrest duration (Fig. 3B). Thus, increased levels of the truncated Cdc20 M43 isoform are sufficient to promote mitotic slippage even in the presence of full-length Cdc20.

Reciprocally, we evaluated whether abrogating expression of the truncated Cdc20 proteoforms affects mitotic arrest timing. Both HeLa cells and the osteosarcoma U2OS cell line undergo mitotic slippage due to Cdc20-mediated APC/C activation (Extended Fig. 6A) and express the truncated Cdc20 proteoforms (Extended Fig. 6B). However, U2OS cells display a substantially shorter mitotic arrest duration than HeLa cells (Extended Fig. 6A), consistent with prior work [29]. RNAi-based replacements with a Cdc20 M43L M88L mutant to prevent expression of the truncated proteoforms resulted in a significant increase in the mitotic arrest duration for each cell line (Fig. 3C). This increased arrest behavior depends upon SAC signaling, as combining the Cdc20 M43L M88L mutant with an R132A mutation to abrogate MCC formation reduced the mitotic arrest duration to 210 min (Extended Fig. 6C). Long-term conditional replacement with the *CDC20 M43L M88L* construct resulted in a growth disadvantage in a competitive proliferation assay with wild-type *CDC20* (Extended Fig. 6D), suggesting that the shorter Cdc20 proteoforms are required for optimal proliferation even in unperturbed cells. We note that, across different cell lines, changes in the levels of other SAC components or their regulatory control may further alter a cell's mitotic arrest duration [1,30,31]. Overall, these results support a model in which the relative levels of Cdc20 proteoforms influence the mitotic arrest duration and cellular fitness of individual cells.

Changes in Cdc20 proteoform levels

Cancer cell lines vary widely in their mitotic arrest duration in the presence of anti-mitotic drugs [29,32], for example with a shorter mitotic arrest duration in U2OS cells compared to HeLa cells (Extended Fig. 6A). Consistent with our model that the relative levels of Cdc20

proteoforms influence mitotic arrest behavior, Western blot analysis of synchronized cells indicated that mitotically-arrested U2OS cells express higher relative levels of the truncated Cdc20 M43 isoform (Fig. 4A), despite the absence of genetic changes within the Cdc20 coding sequence (data not shown). Given the sub-optimal translational context surrounding the M1 start site (Fig. 1E, G), we evaluated whether changes in the translation initiation machinery could alter Cdc20 proteoform levels. The translation initiation factor eIF1 plays a key role in the stringency of translation start site selection [33,34]. In HeLa cells, eIF1 overexpression resulted in a shift in the relative abundance of the full-length and Cdc20 M43 isoforms, with increased levels of the shorter Cdc20 isoform (Extended Fig. 6E). Thus, conditions where the translational machinery is altered, such as between different cell lines, have the potential to modulate Cdc20 proteoform ratios.

We next evaluated changes in the relative Cdc20 proteoform levels over the course of the cell cycle (Fig. 4B; Extended Fig. 7A). Cells enter mitosis with high levels of full-length Cdc20. However, during an extended mitotic arrest, the levels of the full-length protein become reduced with a concomitant increase in the relative level of the M43 isoform. Although this trend is observed for both HeLa and U2OS cells, the full-length:M43 ratio is lower in U2OS cells at mitotic entry and rapidly decreases as cells remain arrested in mitosis (Fig. 4B; Extended Fig. 7A). This change in the relative amount of truncated Cdc20 proteoforms during an extended mitotic arrest is also observed for APC/C-bound Cdc20 based on immunoprecipitation experiments (Fig. 4C, Extended Fig. 7B).

Cdc20 is actively turned over during mitosis through combined protein degradation and synthesis [18]. Thus, the changes in Cdc20 proteoform ratio during a prolonged mitotic arrest could reflect altered protein translation or differential proteoform stability. In mitotically-arrested U2OS cells treated with the proteasome inhibitor MG-132 to assess new Cdc20 translation, the levels of both the full-length and M43 isoforms increased in a manner that depended on new protein synthesis (Extended Fig. 7D). Similarly, mitotic U2OS cells treated with cycloheximide to prevent new protein synthesis display degradation of both the full-length and M43 isoforms (Fig. 4D). However, full-length Cdc20 was eliminated more rapidly leading to increased relative levels of the M43 isoform (Fig. 4D). Degradation of both Cdc20 proteoforms depended on proteasome activity and was suppressed by MG-132 (Extended Fig. 7E). Consistent with a model in which increased M43 isoform levels promote mitotic slippage, we observed a substantial increase in mitotic exit within several hours in cycloheximide-treated cells, but not for synchronized control cells (Fig. 4D, Extended Fig. 7F). However, we note that this may also reflect the combined effect of changes in the translation and degradation of other mitotic factors, such as cyclin B [32,35-37]. We also found that Cdc20 degradation and synthesis rates were faster in U2OS cells relative to HeLa cells (Fig. 4E), suggesting variability in Cdc20 proteoform stability and turnover between cancer cell lines. Together, these results suggest that new protein synthesis and differential Cdc20 isoform turnover during an extended mitotic arrest result in a gradual increase in relative M43 isoform levels with mitotic exit occurring once the truncated M43 isoform achieves sufficient levels.

Cdc20 proteoforms alter drug sensitivity

Anti-mitotic drugs, such as paclitaxel (taxol), other taxanes, and vinca alkaloids, are widely used frontline chemotherapeutics for the treatment of breast cancer, ovarian cancer, and other cancer types [38,39]. However, cancer cells vary widely in their responses to anti-mitotic chemotherapeutics and their ability to escape from the prolonged mitotic arrest induced by treatment with these compounds [29,32]. This mitotic arrest behavior has important implications for anti-mitotic drug efficacy [40], with prior work suggesting that mitotic slippage limits the ability of anti-mitotic drugs to kill cancer cells [40,41]. Indeed, we observed that M1-stop mutant cells, which undergo rapid mitotic slippage in the presence of STLC (Fig. 2D), displayed increased cell viability relative to control cells at higher doses of anti-mitotic drugs (Fig. 5A; Extended Fig. 8A).

As the relative Cdc20 proteoform levels influence mitotic arrest duration (Fig. 3A-C), we sought to test the effect of these changes on anti-mitotic drug sensitivity. Mitotically-enriched HeLa cells display a 5.4:1 ratio of Cdc20 full-length:M43 (Fig. 5B). To modulate Cdc20 proteoform ratios, we generated clonal cell lines expressing varying levels of the wild-type *CDC20* cDNA in the M1-stop mutant cell line, which lacks full-length Cdc20 (Extended Fig. 8B-C). Our analysis revealed a close correlation between the relative Cdc20 proteoform ratio, mitotic arrest duration, and anti-mitotic drug sensitivity (Fig 5B-D, Extended Fig 8D-E), with an increased ratio of full-length Cdc20 resulting in a persistent mitotic arrest and significantly increased sensitivity to high STLC levels. Clones expressing an intermediate ratio of full-length Cdc20 protein (2.6:1) displayed intermediate drug sensitivity and a variable mitotic arrest behavior (Fig. 5C-D), likely reflecting stochastic differences in Cdc20 expression in individual cells. RNAi-based depletion of the endogenously-expressed truncated Cdc20 proteoforms (thereby increasing the relative level of full-length Cdc20) suppressed this heterogeneous mitotic arrest behavior (Extended Fig. 8E). Together, our results indicate that, within a given cell line, the relative levels of Cdc20 proteoforms modulate both mitotic arrest timing and anti-mitotic drug sensitivity.

Through a survey of tumors and cancer cell lines using public databases, we identified multiple distinct genetic mutations within *CDC20* that are predicted to eliminate the full-length Cdc20 protein, thus increasing the relative levels of the truncated proteoforms (Fig. 5E). We focused our analysis on the endometrial adenocarcinoma HEC-6 cell line, which our sequencing analysis confirmed contains a heterozygous nonsense mutation (Q3-stop) at the *CDC20* locus (Fig. 5F). As predicted from this mutation, the HEC-6 cell line displayed a substantial reduction in the relative levels of full-length Cdc20, with a corresponding increase in the M43 and M88 isoforms (Fig. 5G). HEC-6 cells showed a substantially reduced mitotic arrest duration in the presence of STLC relative to HeLa cells (Fig. 5H). This reduced mitotic arrest duration was suppressed by inhibiting the APC/C with proTAME (Extended Fig. 8F). HEC-6 cells were also more sensitive to APC/C inhibition in the absence of STLC treatment, displaying delayed mitotic progression even at proTAME concentrations where HeLa cells are largely unaffected (Extended Fig. 8G). RNAi-based replacements with the wild-type *CDC20* cDNA in HEC-6 cells resulted in increased relative levels of full-length Cdc20 (Fig. 5I) and a concomitant increase in the mitotic arrest duration (Fig. 5J). In contrast, replacement with a ΔM1 mutant abrogated expression of

the full-length Cdc20 protein and resulted in a further reduction in the mitotic arrest duration (Fig. 5J). The mitotic arrest behavior of the ΔM1 mutant was dependent on the Cdc20 M43 isoform (Extended Fig. 8H). Importantly, the relative Cdc20 proteoform ratio also correlated with anti-mitotic drug sensitivity. Control HEC-6 cells or cells expressing only the *CDC20-ΔM1* mutant cDNA were more resistant to high concentrations of STLC compared to HeLa cells (Fig. 5A, 5K). However, replacement with the wild-type *CDC20* cDNA resulted in significantly increased drug sensitivity (Fig. 5K), demonstrating that drug resistance can be reversed by restoring normal Cdc20 proteoform ratios.

A Tunable Mitotic Arrest Timer

Our findings reveal a mechanism to control mitotic arrest duration based on the presence of alternative Cdc20 translational isoforms that are resistant to SAC-mediated inhibition. When exposed to continuous mitotic perturbations, a given human cell line will arrest for a defined period of time (for example, ~30 hours in HeLa cells) before undergoing premature mitotic exit (mitotic slippage) without segregating their chromosomes. The presence of multiple Cdc20 proteoforms within the same cell provides an explanation for how cells create a tunable mitotic arrest timer. We propose a model in which changes in the Cdc20 proteoform levels occur in arrested cells due to differential protein turnover (Fig. 4B, 4D), acting as an elegant molecular timer to directly tune mitotic arrest duration. First, the Cdc20 locus is decoded into multiple translational isoforms (Fig. 1C) that display differential sensitivity to SAC inhibition (Fig. 2D-E). Second, at the beginning of mitosis, the M1 Cdc20 proteoform dominates (Fig. 4B, Extended Fig. 7A), ensuring that the SAC can effectively inhibit the APC/C and prevent mitotic exit. Third, during an extended mitotic arrest, the combination of ongoing protein synthesis and proteasome-dependent degradation with an increased degradation rate for the M1 isoform (Fig. 4D-E, Extended Fig. 7D-E) result in a gradual increase in relative M43 isoform levels (Fig. 4B, Extended Fig. 7A). Fourth, when M43 levels reach a threshold proportion of total Cdc20 protein, it will activate enough APC/C complexes to trigger mitotic exit even in the presence of continued SAC activation (Fig. 4B, 4D, Extended Fig. 7A). These predictions are supported by multiple perturbations and conditions that alter the relative proteoform ratios or new protein synthesis (see Extended Fig. 9). Although our work suggests that the presence of these Cdc20 proteoforms is central to understanding the physiological mitotic arrest behavior of human cells and creating a mitotic arrest timer, the overall arrest behavior will reflect the integration of multiple signals and regulatory pathways. Prior work has identified additional factors that can act to modulate this mitotic arrest timer, such as cyclin B levels, or the extent and persistence of mitotic checkpoint activation [1,2].

Alternative translation initiation has been observed for diverse proteins in eukaryotic cells with the potential to create distinct proteoforms [42-45], but there are only limited examples of alternative translation playing roles in cell cycle control [46]. Our work provides a paradigm for the contributions of functional alternative translational isoforms in modulating cell cycle events through changes to a critical regulatory domain. Genetic mutations, translational differences, or changes in Cdc20 protein degradation rate that influence the relative Cdc20 proteoform levels would affect mitotic arrest timing, anti-mitotic drug sensitivity, and cancer cell behavior.

Methods

Cell culture and reagents

HeLa, hTERT-RPE1, U2OS, A549, DLD-1, and NIH/3T3 cell lines were cultured in Dulbecco's modified Eagle medium (DMEM) supplemented with 10% fetal bovine serum (FBS), 100 U/mL penicillin and streptomycin, and 2 mM L-glutamine at 37°C with 5% CO_2. The HEC-6 cell line was cultured in DMEM supplemented with 15% FBS and 2 mM L-glutamine. Doxycycline-inducible cell lines were cultured in medium containing FBS certified tetracycline-free. spCas9 expression in inducible CRISPR/Cas9 cell lines was induced with 1 μg/ml doxycycline hyclate (Sigma) at 24 hr intervals for 2 days. All other doxycycline-inducible constructs were induced with 10 ng/ml doxycycline hyclate, unless indicated in figure legend. Other drugs used on human cells were Nocodazole (Sigma, 330 nM), S-trityl-L-cysteine (STLC; Sigma, 10 μM unless otherwise indicated), Paclitaxel (Taxol; Invitrogen, 1 μM), GSK923295 (CENP-E inhibitor; Selleck Chemicals, 100 nM), proTAME (APC/Ci; R&D Systems, 12 μM), AZ-3146 (Mps1i; Selleck Chemicals, 4 μM), cycloheximide (CHX; Sigma, 50 μg/ml), MG-132 (MG132; Enzo Life Sciences, 10 μM) unless concentration indicated otherwise in figure legend. Cells were enriched in mitosis with treatment with 330 nM nocodazole for 16-17 hrs or if indicated, 10 μM STLC for 18 hrs. The antibodies used in this study are described in the relevant methods and in Supplementary Table 1.

Cell line generation

The cell lines used in this study are described in Supplementary Table 2. The parental HEC-6 cell line was obtained from JCRB Cell Bank. All other parental cell lines are from Cheeseman Lab stocks. Cell lines were regularly tested for mycoplasma contamination.

The inducible CRISPR/Cas9 HeLa cell line was previously generated by transposition as described [7]. A control sgRNA (Ctrl sgRNA, GCCGATGGTGAAGTGGTAAG) or sgRNAs targeting different regions within the *CDC20* gene (sgM1, TCGAACGCGAACTGTGCCAT; sgExon1, CCTGCACTCGCTGCTTCAGC; sgExon3, CCAGGAACATCAGAAAGCCT) were cloned into the sgOpti plasmid (puro-resistant, Addgene #85681) and introduced into the inducible CRISPR/Cas9 HeLa cell line by lentiviral transduction [7]. Cells were selected with 0.5 μg/ml puromycin (Gibco) for 5 days.

Stable clonal cell lines lacking the canonical full-length Cdc20 protein were obtained by transfecting HeLa cells with pX330-based plasmids [47] expressing spCas9 and either the sgM1 (for ΔM1 mutant) or the sgExon1 guide RNA (for M1-stop mutant). pX330-based plasmids were transfected using X-tremeGENE-9 (Roche) together with a mCherry-expressing plasmid. Single mCherry-positive cells were fluorescence activated cell-sorted into 96-well plates. Clones were screened for successful gene editing and the nucleotide sequence of the *CDC20* alleles were determined by next-generation sequencing (Genewiz Amplicon-EZ).

pBABE derivatives containing empty IRES_EGFP or different Cdc20_IRES2_EGFP constructs were transfected with Effectene (Qiagen) along with a VSVG packaging plasmid into 293-GP cells for generation of retrovirus as described [48]. Supernatant containing

retrovirus was sterile-filtered, supplemented with 20 μg/mL polybrene (Millipore), and used to transduce inducible CRISPR/Cas9 HeLa cells expressing the sgExon3 guide RNA. At two days post-transduction, cells were selected with 375 μg/ml hygromycin (Invitrogen) for 10-14 days.

Doxycycline-inducible cell lines were generated by homology-directed insertion into the *AAVS1* "safe-harbor" locus. Donor plasmid containing a selection marker, the tetracycline-responsive promoter, the transgene as indicated, and reverse tetracycline-controlled transactivator flanked by *AAVS1* homology arms [49] was transfected into the indicated cell line using Effectene (Qiagen) according to the manufacturer's protocol with a pX330-based plasmid [47] expressing both spCas9 and a guide RNA specific for the *AAVS1* locus (GGGGCCACTAGGGACAGGAT). At two days post-transduction, cells were selected with hygromycin (375 μg/ml for HeLa and its derivatives or 100 μg/ml for U2OS) for 10-14 days.

Lentiviral plasmids containing mEGFP only or *CDC20(WT)* or *CDC20-ΔM1* or *CDC20-ΔM1 M43L* under the control of the UbC promoter were introduced into the HEC-6 cell line by lentiviral transduction. Lentivirus was removed from cells at 4 hrs post-spinfection. At two days post-transduction, cells were selected with 0.25 μg/ml puromycin (Gibco) for 4 days.

RNAi treatment and gene replacements

Custom siRNAs against Cdc20 (5'-CGGAAGACCUGCCGUUACAUU), Cdh1 (5'-UGAGAAGUCUCCCAGUCAG), and Mad2 (5'- UACGGACUCACCUUGCUUGUU) and a non-targeting control pool (D-001206-13) were obtained from Dharmacon. siRNAs were applied at a final concentration of 50 nM, unless indicated in the figure legend. 2.5 μl Lipofectamine RNAiMAX (Invitrogen) was used per ml of final transfection medium. For gene replacements, transfection medium also contained the appropriate concentration of doxycycline hyclate to express the ectopic inducible construct. Transfection medium was changed after 6 hrs for time-lapse microscopy analyses and competitive proliferation assays and either 6 hrs or 20 hrs for Western blot analyses.

Immunofluorescence microscopy

Cells for immunofluorescence were seeded on poly-L-lysine (Sigma) coated coverslips and treated with 330 nM nocodazole for 1.5 hr before pre-extraction and fixation. Cells were pre-extracted in PBS + 0.2% Triton X-100 for 1 min at 37°C before fixation with PBS + 0.2% Triton X-100 + 4% formaldehyde at room temperature for 10 min. Coverslips were washed with PBS + 0.1% Triton X-100 and blocked in Abdil (20 mM Tris-HCl pH 7.5, 150 mM NaCl, 0.1% Triton X-100, 3% BSA, 0.1% NaN_3) for 30 min. Immunostaining was performed by incubating coverslips with primary antibodies diluted in Abdil for 45 min at room temperature followed by 3 consecutive washes with PBS + 0.1% Triton X-100. Cy2- and Cy5-conjugated secondary antibodies (Jackson ImmunoResearch Laboratories) were diluted 1:500 in Abdil together with 0.3 μg/ml Hoechst-33342 (Invitrogen) and incubated with coverslips for 45 min. After washing with PBS + 0.1% Triton X-100, coverslips were mounted with ProLong Gold Antifade (Invitrogen) and allowed to cure overnight before imaging.

The following primary antibodies were used: anti-centromere antibodies, ACA (1:200, Antibodies Inc, #15-234), Mad2 (1:1,000, Kops Lab [50]), Bub1 (1:200, Abcam, ab54893). Images were acquired on a DeltaVision Core deconvolution microscope (Applied Precision) equipped with a CoolSnap HQ2 charge-coupled device camera and deconvolved where appropriate using the Softworx software. Z-sections were acquired at 0.2 μm steps using a Plan Apo 100X/1.4 NA objective and appropriate fluorescence filters. Image analysis was performed in Fiji (ImageJ, NIH).

Western blots

Cells were treated with 330 nM nocodazole or 10 μM STLC for 16-18 hrs before harvesting for Western blot analysis. Cells were washed with PBS and immediately lysed on ice for 30 min in fresh urea lysis buffer (50 mM Tris pH 7.5, 150 mM NaCl, 0.5% NP-40, 0.1% SDS, 6.5 M Urea, 1X Complete EDTA-free protease inhibitor cocktail (Roche), 1 mM PMSF). Cellular debris were removed by centrifugation. Protein concentrations in each sample were measured using either Bradford reagent (Bio-Rad) or Non-Interfering protein assay (G-Biosciences), and sample concentrations were normalized by addition of Laemmli sample buffer. Lysates were heated at 95°C for 5 min, separated by SDS-PAGE on a 10% acrylamide gel, and transferred to PVDF membrane (GE Healthcare or EMD Millipore).

For standard chemiluminescence, membrane was blocked for 1 hr in Blocking Buffer (2% milk in PBS + 0.05% Tween-20). Primary antibodies were diluted in 0.2% milk in PBS + 0.05% Tween-20 +/− 0.2% NaN_3 and applied to the membrane overnight at 4°C or for 1-2 hrs at room temperature. HRP-conjugated secondary antibodies (GE Healthcare or Kindle Biosciences) were diluted in 0.2% milk in PBS + 0.05% Tween-20 and applied to the membrane for 1 hr at room temperature. After washing in PBS + 0.05% Tween-20, Clarity enhanced chemiluminescence substrate (Bio-Rad) was added to the membrane according to the manufacturer's instructions. Membrane was imaged with a KwikQuant Imager (Kindle Biosciences) and analyzed using Adobe Photoshop and LI-COR Image Studio software.

For quantitative Western blotting, the membrane was blocked for 1 hr in Intercept® (PBS) Blocking Buffer (LI-COR). Primary antibodies were diluted in Intercept® (PBS) Blocking Buffer + 0.05% Tween-20 and applied to the membrane for 1-2 hrs at room temperature. IRDye® 800CW Goat anti-mouse and/or IRDye® 680RD Goat anti-rabbit secondary antibodies (LI-COR) were diluted in Intercept® (PBS) Blocking Buffer + 0.1% Tween-20 and applied to the membrane for 1 hr at room temperature. Membrane was imaged with the Odyssey® CLx Imager (LI-COR) and analyzed using LI-COR Image Studio software.

The following primary antibodies were used: C-terminus (aa 450-499) of human Cdc20 (C-term Ab, 1:500, Abcam, ab26483), N-terminus (aa 1-175) of human Cdc20 (N-term Ab, 1:300, Santa Cruz Biotechnology, sc-13162), antibody raised against acetylated M88-terminus of human Cdc20 (M88Ac Ab, 1:40,000, Cheeseman Lab), GFP (1:1,000, Roche, 11814460001), APC7 (1:2,000, Bethyl Laboratories, A302-551A), Bub3 (1:1,000, BD Biosciences, 611730), GAPDH (1:10,000, Cell Signaling Technology, #2118), GAPDH (1:20,000, Abcam, ab185059, HRP-conjugated), β-actin (1:20,000, Santa Cruz

Biotechnology, sc-47778, HRP-conjugated). The uncropped original images of all Western blots in this study are provided in Supplementary Figure 1.

Lambda phosphatase treatment

HeLa cells were treated with 330 nM nocodazole overnight and mitotic cells were harvested by shake-off. Cells were washed with PBS and then lysed on ice for 45 min in HEPES/Triton X-100 lysis buffer (20 mM HEPES pH 7.5, 150 mM NaCl, 1% Triton X-100, 5 mM $MgCl_2$, 1X Complete EDTA-free protease inhibitor cocktail (Roche), 1 mM PMSF). Cellular debris was removed by centrifugation and the resulting lysate was split into three parts. One sample was left untreated and the other two were supplemented with 1X Protein MetalloPhosphatase buffer (New England Biolabs) and 1 mM $MnCl_2$ only or together with 1 μl Lambda Protein Phosphatase (New England Biolabs). After incubation at 30°C for 30 min, reactions were stopped by addition of 2X Laemmli sample buffer and heated at 95°C for 5 min. Samples were analyzed by SDS-PAGE and Western blot.

Time-lapse experiments for mitotic timing

Cells were first seeded in 12-well polymer-bottomed plates (Cellvis, P12-1.5P) and treated as indicated in the figure legends. Cells were later moved to CO_2-independent media (Gibco) supplemented with either 10% FBS or 15% FBS for HEC-6 derived cell lines, 100 U/mL penicillin and streptomycin, and 2 mM L-glutamine before imaging at 37°C. Phase contrast images were acquired on a Nikon eclipse microscope equipped with a charge-coupled device camera (Clara, Andor) or a sCMOS camera (ORCA-Fusion BT, Hamamatsu) using a Plan Fluor 20X/0.5 NA objective at either 2 min, 5 min, or 10 min intervals. Time-lapse movies were analyzed using Fiji (ImageJ, NIH), ilastik [51] and CellProfiler [52]. Image brightness and contrast were first adjusted in Fiji. Pixel-based classification was performed on individual images using ilastik and the resulting probability map images were processed by CellProfiler to identify and track mitotic cells. Each mitotic cell was then confirmed manually and the mitotic duration was determined as the time from cell rounding at mitotic entry to cell flattening after mitotic exit.

Live-cell fluorescence imaging

For live-cell fluorescence imaging, cells were seeded into 8-well glass-bottomed chambers (Ibidi or Cellvis) and moved into CO_2-independent media (Gibco) before imaging at 37°C. DNA was stained with 0.2 μg/ml Hoechst-33342 (Invitrogen). Cells were imaged directly or after 1 hr incubation with 330 nM nocodazole. Images were acquired on a DeltaVision Core deconvolution microscope (Applied Precision) equipped with a CoolSnap HQ2 charge-coupled device camera and deconvolved using the Softworx software. Z-sections were acquired at 0.5 μm steps using a Plan Apo 100X/1.4 NA objective and appropriate fluorescence filters. Image analysis was performed in Fiji (ImageJ, NIH).

Mitotic index analysis

To determine the mitotic index from microscope images, cells were seeded in 12-well polymer-bottomed plates (Cellvis, P12-1.5P) and treated as indicated in the figure legends before fixing in PBS + 4% formaldehyde for 10 min at room temperature. After washing

with PBS, cells were incubated in Abdil containing 0.5 μg/ml Hoechst-33342 (Invitrogen) for 30 min. Cells were washed with PBS and stored in Abdil until ready to image. Images were acquired on a Nikon eclipse microscope equipped with a charge-coupled device camera (Clara, Andor) using a Plan Fluor 20X/0.5 NA objective and appropriate fluorescence filters. Image analysis was performed in Fiji (ImageJ, NIH). The mitotic index was determined by scoring the number of mitotic cells with condensed DNA and dividing by the total number of cells.

For the analysis of the mitotic index using flow cytometry, cells were collected by incubation for 10 min in PBS + 5 mM EDTA, washed once in PBS, then fixed in PBS + 2% formaldehyde for 10 min at room temperature. After washing with PBS + 0.1% Triton X-100, cells were first immunostained for histone H3 phosphorylated at serine residue 10 (H3pS10 Ab, 1:3,000, Abcam, ab5176) diluted in Abdil, followed by AlexaFluor 647-conjugated secondary antibody (Jackson ImmunoResearch Laboratories). The proportion of GFP-positive single cells also staining positive for H3pS10 was determined on an LSR Fortessa (BD Biosciences) flow cytometer and analyzed with FlowJo software. High levels H3pS10 were used as a marker of mitosis. At least 550 GFP-positive cells were analyzed per condition.

Evolutionary conservation analysis

Protein sequences of Cdc20 orthologs from the following tetrapod species were aligned using COBALT [53]: *Homo sapiens* (Human, NP_001246.2), *Macaca mulatta* (Rhesus, NP_001248046.1), *Mus musculus* (Mouse, NP_075712.2), *Canis lupus familiaris* (Dog, XP_003639578.1), *Loxodonta africana* (Elephant, XP_023410383.1), *Gallus gallus* (Chicken, NP_001006536.1), and *Xenopus tropicalis* (Xenopus, NP_988945.1). For the altORF conservation analysis, the DNA sequence of canonical open-reading frames (ORFs) from all mammalian species with orthologs to human *CDC20* (ENSG00000117399) were obtained from Ensembl Release 103 [54]. For species with multiple orthologous transcripts, only one ORF sequence (the most conserved relative to human) was used. An ORF analysis was performed to identify start and stop codons in 2 forward frames and visualized for the first 300 nt.

GFP immunoprecipitation and Mass Spectrometry

IP-MS experiments were performed as described previously [55]. Eluted proteins from control HeLa heterozygous cells with one CDC20 allele tagged with a C-terminal mEGFP tag at the endogenous locus were digested with mass-spectrometry grade Lys-C and trypsin (Promega). Due to the presence of neighboring arginine residues and to maximize the identification of alternative isoforms, proteins eluted from a cell line derived from the tagged cell line above but lacking full-length Cdc20 (*CDC20*_M1-fs-M43, Extended Fig. 2A) were digested with Lys-C alone. Both cell lines were enriched in mitosis using nocodazole only for control cells or double thymidine synchronization followed by nocodazole treatment for the *CDC20*_M1-fs-M43 cell line.

Harvested cells were washed in PBS and resuspended 1:1 in 1X Lysis Buffer (50 mM HEPES pH 7.4, 1 mM EGTA, 1 mM $MgCl_2$, 100 mM KCl, 10% glycerol) then drop frozen

in liquid nitrogen. Cells were thawed after addition of an equal volume of 1.5X lysis buffer supplemented with 0.075% NP-40, 1X Complete EDTA-free protease inhibitor cocktail (Roche), 1 mM PMSF, 20 mM beta-glycerophosphate, and 0.4 mM sodium orthovanadate. Cells were lysed by sonication and cleared by centrifugation. The supernatant was mixed with Protein A beads coupled to rabbit anti-GFP antibody (Cheeseman lab) and rotated at 4°C for 1 hr. Beads were washed five times in Wash Buffer (50 mM HEPES pH 7.4, 1 mM EGTA, 1 mM $MgCl_2$, 300 mM KCl, 10% glycerol, 0.05% NP-40, 1 mM DTT, 10 μg/mL leupeptin/pepstatin/chymostatin). After a final wash in Wash Buffer without detergent, bound protein was eluted with 100 mM glycine pH 2.6. Eluted proteins were precipitated by addition of $1/5^{th}$ volume trichloroacetic acid at 4°C overnight. Precipitated proteins were reduced with TCEP, alkylated with iodoacetamide, and digested with mass-spectrometry grade Lys-C and trypsin or Lys-C alone (Promega). Digested peptides were separated by liquid chromatography and analyzed on an Orbitrap Elite mass spectrometer (Thermo Fisher). Data were analyzed using Proteome Discover Software (Thermo Fisher).

Immunoprecipitation and Western blot

For the GFP IP-Western experiments, the different mEGFP constructs were induced with doxycycline and cells were arrested in mitosis with STLC treatment for 6 hrs before harvest by mitotic shake-off. For the APC/C IP-Western experiments, U2OS cells were first arrested in S phase using 2.5 mM thymidine (Sigma) for 25-26 hrs and then washed and released into medium without thymidine supplemented with STLC for 15 hrs (short mitotic arrest) or 22 hrs (long mitotic arrest). Alternatively, HeLa cells were treated with STLC for 6 hrs (short mitotic arrest) or 16 hrs (long mitotic arrest). Mitotically-arrested cells were collected by shake-off and processed for immunoprecipitations.

Harvested cells were washed in ice-cold PBS, then lysed on ice for 20 min in Lysis Buffer (50 mM HEPES, 1 mM EGTA, 1 mM $MgCl_2$, 100 mM KCl, 10% glycerol, 0.5% NP-40, 1 mM dithiothreitol, 1X Complete EDTA-free protease inhibitor cocktail (Roche), 1 mM PMSF, 20 mM β-glycerophosphate, 0.5mM sodium fluoride, and 0.5 mM sodium orthovanadate, pH 7.4). Cellular debris was removed by centrifugation. Protein concentrations in each sample were measured using Bradford reagent (Bio-Rad), and sample concentrations were normalized before addition of Protein A beads (Bio-Rad) coupled to either affinity-purified rabbit anti-GFP polyclonal antibodies (Cheeseman lab) or affinity-purified mouse anti-CDC27/APC3 monoclonal antibodies (BD 610455). After 1 hr incubation at 4°C, beads were washed 4X with Wash Buffer (50 mM HEPES, 1 mM EGTA, 1 mM MgCl2, 100 mM KCl, 10% glycerol, 0.05% NP-40, 1 mM dithiothreitol, 10 μg/mL leupeptin/pepstatin/chymostatin, pH 7.4). Beads were then incubated in 2X volume of Laemmli buffer for 5 min at 95°C to remove bound protein. Samples were analyzed by SDS-PAGE and Western blotting as described above.

Competitive proliferation assay with long-term conditional Cdc20 replacement

BFP-expressing HeLa cells with an ectopic siRNA-resistant *CDC20(WT)* construct were mixed 1:1 with mCherry-expressing HeLa cells with similar *CDC20(WT)* or *CDC20(M43L M88L)* constructs. Endogenous Cdc20 protein was depleted by siRNA transfection as described above. After the first siRNA transfection, cells were transfected every 3-4 days

and passaged 2-3 days after every siRNA transfection for 24 days. Proliferation of the BFP- and mCherry-expressing cells was monitored by flow cytometry on an LSR Fortessa (BD Biosciences) flow cytometer and analyzed with FlowJo software. The percentage of mCherry-positive cells at the indicated timepoint was quantified and normalized to the initial levels determined two days after the first siRNA transfection.

eIF1 over-expression with cell synchronization

EGFP alone or EGFP-eIF1 overexpression was induced in HeLa cells with 1 μg/ml doxycycline for 24 hrs before cells were arrested in S phase using 2.5 mM thymidine (Sigma). After 24 hrs thymidine arrest, cells were release into medium without thymidine supplemented with doxycycline and 10 μM STLC to arrest cells in mitosis. Mitotically-arrested cells were collected by shake-off at 16 hrs post-release and analyzed by SDS-PAGE and western blot. Cdc20 isoform levels in serial diluted lysates were quantified for the full-length and M43 isoforms from short exposure and long exposure images respectively with antibodies recognizing the two Cdc20 isoforms. The levels in the undiluted HeLa sample expressing GFP alone (40 μg) were set to 1.

Cell synchronization using double thymidine arrest

HeLa and U2OS cells were first arrested in S phase using 2.5 mM thymidine (Sigma) for 22-23 hrs and then washed and released into medium without thymidine for 10 hrs. Cells were then arrested a second time in S phase using 2.5mM thymidine for another 12-13 hrs before finally washing and releasing them into medium without thymidine supplemented with STLC to arrest cells in mitosis. Synchronized cells were harvested at various time points after the second thymidine release and analyzed by SDS-PAGE and quantitative Western blot using LI-COR as described above. The protein levels of full-length Cdc20 or the M43 isoform were quantified at the indicated time points and the ratio was calculated.

Drug treatments for protein synthesis or protein degradation

U2OS cells were first arrested in S phase using 2.5 mM thymidine (Sigma) for 26 hrs and then washed and released into medium without thymidine supplemented with STLC to arrest cells in mitosis. Mitotically-arrested cells were collected by shake-off at 21-22 hrs post-release (prolonged mitotic arrest) and treated with either cycloheximide (final concentration 50 μg/ml) to inhibit new protein synthesis, MG-132 (final concentration 10 μM) to inhibit proteasome-mediated degradation, or both cycloheximide and MG-132 to inhibit both new protein synthesis and protein degradation. Cells were harvested at various time points after drug addition, washed once with ice-cold PBS supplemented with the appropriate drug(s), and analyzed by SDS-PAGE and either western blot or quantitative western blot using LI-COR as described above. The protein levels of full-length Cdc20 or the M43 isoform were quantified at the indicated time points, normalized against the loading control (either β-actin or GAPDH as shown in each figure), and the indicated initial Cdc20 levels were set to 100% or 1.

M88Ac antibody generation

The M88Ac antibody was generated against a synthesized acetylated-peptide with the following amino acid sequence: Ac-MEVASFLLSC (New England Peptide, Covance). Serum from immunized rabbit was depleted against an acetylated spanning peptide (Ac-PHRSAAQMEVASFLC) and affinity-purified against the acetylated peptide.

MTT viability assay

HeLa or M1-stop cells were seeded at a density of 2,000 cells per well in 96-well plates and subsequently cultured for 72 hrs in triplicate with increasing concentrations of the indicated anti-mitotic drug. After 72 hrs incubation, the medium was removed and the cells were stained with 2.5 mg/ml MTT (3-(4,5-dimethylthiazol-2-yl)-2,5-diphenyltetrazolium bromide, Biosynth) in medium without serum for 3 hrs. Formazan crystals formed by the cells were then dissolved in 4 mM HCl and 0.1% NP-40 in isopropanol for 15 min. The absorbance was read at 570 nm on a Multiskan GO plate reader (Thermo Scientific), using 650 nm as reference wavelength.

Representative clonal cell lines expressing varying levels of the wild-type *CDC20* cDNA from an inducible construct in the M1-stop mutant cell line were seeded at a density of 2,000 cells per well in 96-well plates and either cultured uninduced in triplicate or with *CDC20(WT)* induction for 43 hrs with 20 ng/ml. Cells were then cultured for 72 hrs with increasing concentrations of STLC and processed for MTT viability assay as described above.

HEC-6 cell lines expressing either mEGFP alone or *CDC20(WT)* or *CDC20-ΔM1* were seeded in triplicate at a density of 1,500 cells per well in 96-well plates. Cells were transfected with either a non-targeting control siRNA pool for mEGFP-expressing cells (no Cdc20 replacement) or Cdc20 siRNAs for cells expressing *CDC20* constructs. siRNAs were applied as described above with volumes adjusted for 96-well plate format and transfection medium was changed after 6 hrs. At 32 hrs post-transfection, cells were then cultured for 92 hrs with increasing concentrations of STLC and processed for MTT viability assay as described above.

Extended Data

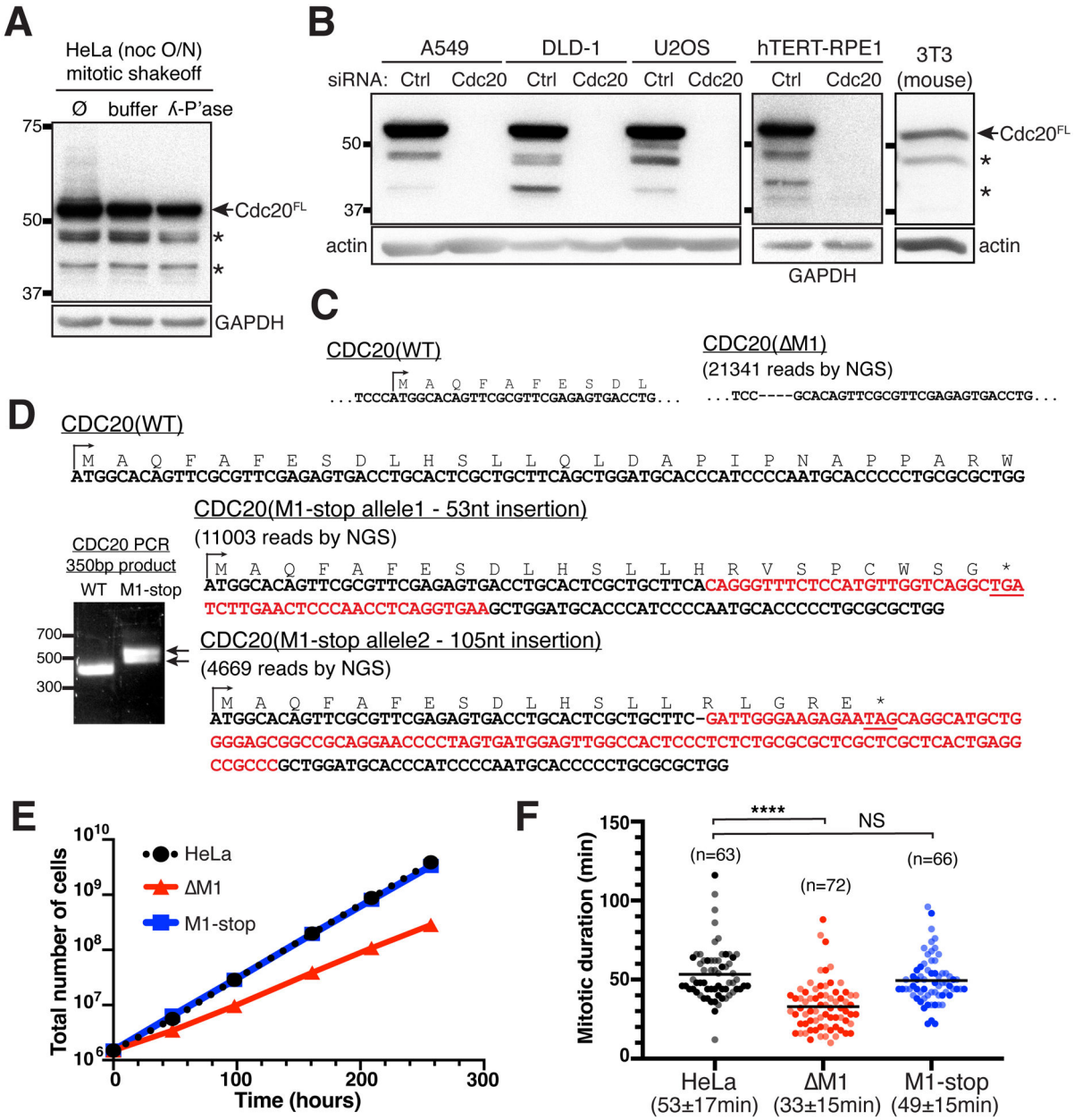

Extended Data Figure 1. Human cells express alternative isoforms of Cdc20. Related to Figure 1.

(**A**) Western blot showing mitotic HeLa cells collected by shake-off after overnight treatment with 330 nM nocodazole. Lysates alone, with buffer only, or with buffer and lambda phosphatase treatment were probed using antibodies recognizing the C-terminus of human Cdc20 (aa 450-499). GAPDH was used as loading control. (**B**) Western blot showing multiple human cancer cell lines (A549, DLD-1, and U2OS) and the non-transformed human hTERT RPE-1 cells treated with control or Cdc20 siRNAs, as well as the mouse NIH/3T3 cell line. Cdc20 protein species were detected with antibodies recognizing the C-terminus of human Cdc20 (aa 450-499). β-actin or GAPDH was used as loading control.

(**C**) Sequence information for the homozygous ΔM1 mutant cell line lacking the canonical M1 ATG start codon. The DNA sequence of the genomic locus was determined by next-generation sequencing. (**D**) Sequence information for the M1-stop mutant cell line showing insertions of 53 nt and 105 nt respectively after the L14 residue. Underlined are premature stop codons that are in-frame with the M1 ATG start codon for both *CDC20* alleles. The DNA sequence of the genomic locus was determined by next-generation sequencing. (**E**) Growth curves of control HeLa compared to the ΔM1 and M1-stop mutant cell lines. (**F**) Graph showing mitotic duration for control HeLa compared to the ΔM1 and M1-stop mutant cell lines. Each point represents a single cell. The bars correspond to the mean. Indicated are the mean mitotic duration ± standard deviation across two experimental replicates, with replicates shaded-coded. The total number of cells analyzed is indicated. Statistics from Student's two-sample t-Test with two-tailed distribution (****$p < 0.0001$, NS not significant).

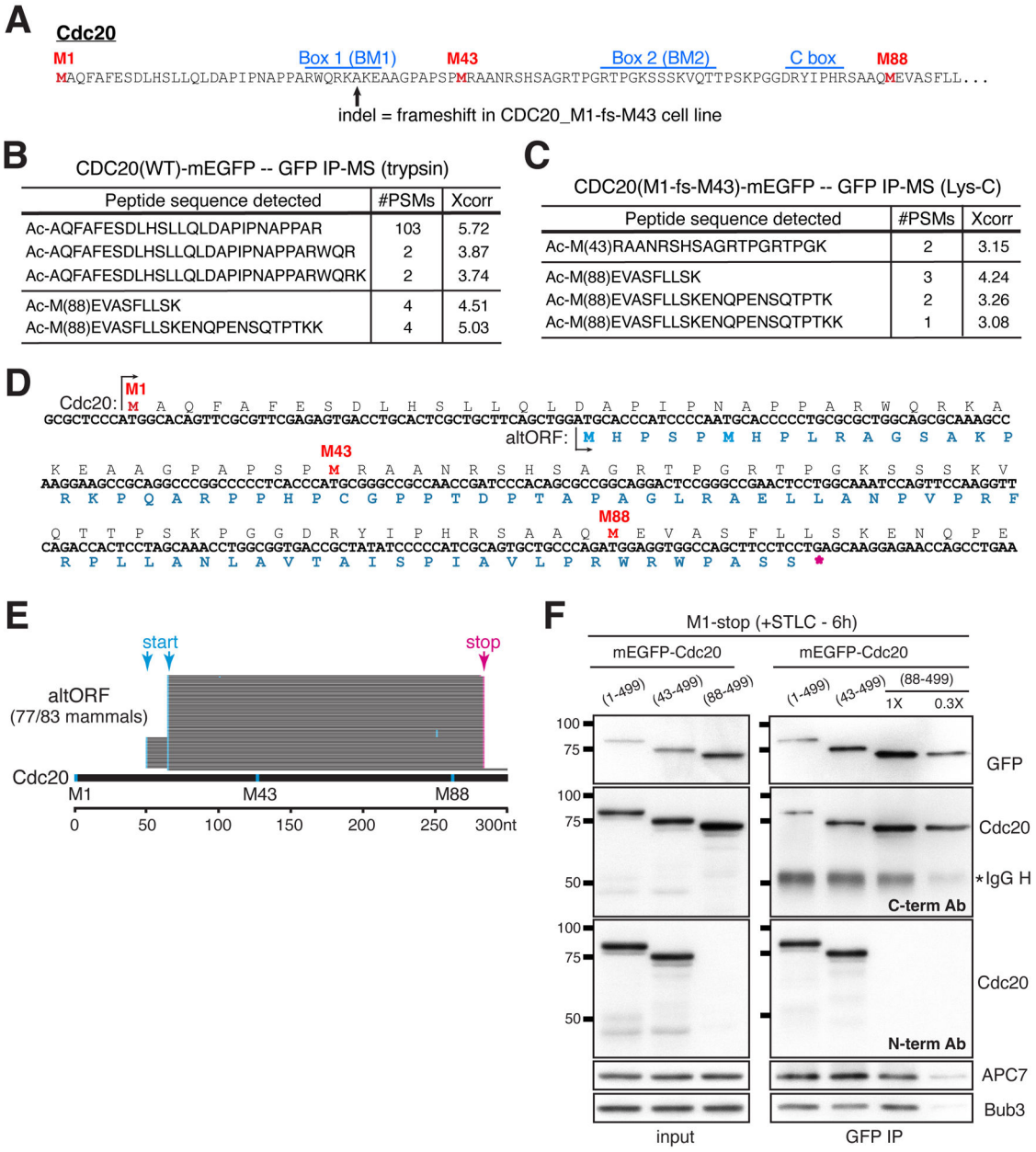

Extended Data Figure 2. Cdc20 isoforms are produced by alternative translation initiation at downstream in-frame start codons. Related to Figure 1.

(**A**) Protein sequence of the N-terminal region of human Cdc20 with conserved motifs indicated. Methionine residues are highlighted in red. Arrow indicates the location of indel mutations in the *CDC20*_M1-fs-M43 cell line. (**B**) Cdc20 tryptic peptides with N-terminal acetylation indicative of translation initiation were identified following GFP immunoprecipitation-mass spectrometry of mitotically-enriched HeLa cells containing one allele of *CDC20* with an endogenous C-terminal mEGFP tag. The identified peptide sequence, number of peptide-spectrum matches (#PSMs), and the cross-correlation (Xcorr) value from the SEQUEST search are indicated. Due to the presence of neighboring arginine residues, we did not detect the Ac-M43 peptide in this tryptic digest. (**C**) Cdc20 peptides

as in (B), except using the endopeptidase LysC alone and isolated using a C-terminal mEGFP tag in a cell line lacking the full-length Cdc20 protein (*CDC20*_M1-fs-M43) to maximize identification of alternative isoforms. (**D**) Analysis of human *CDC20* nucleic acid sequence reveals two alternative out-of-frame start codons between Met1 and Met43. The amino acid sequence of the predicted alternative open reading frame (altORF) is indicated in blue, with the methionines bolded in cyan. Methionine residues are highlighted in red. (**E**) Conservation analysis for the presence of Cdc20 altORF across various mammalian species. The altORF was detected in 77 out of 83 species analyzed. For each species, start and stop codons are mapped relative to human Cdc20 protein sequence and indicated in cyan and magenta respectively. (**F**) Western blot following GFP immunoprecipitation of mEGFP-Cdc20 fusions expressed in mitotically-enriched M1-stop cells. Antibodies against GFP, the C-terminus of Cdc20, the N-terminus of Cdc20, APC7, and Bub3 were used to detect the mEGFP-fusions, endogenous Cdc20, APC/C, and MCC respectively.

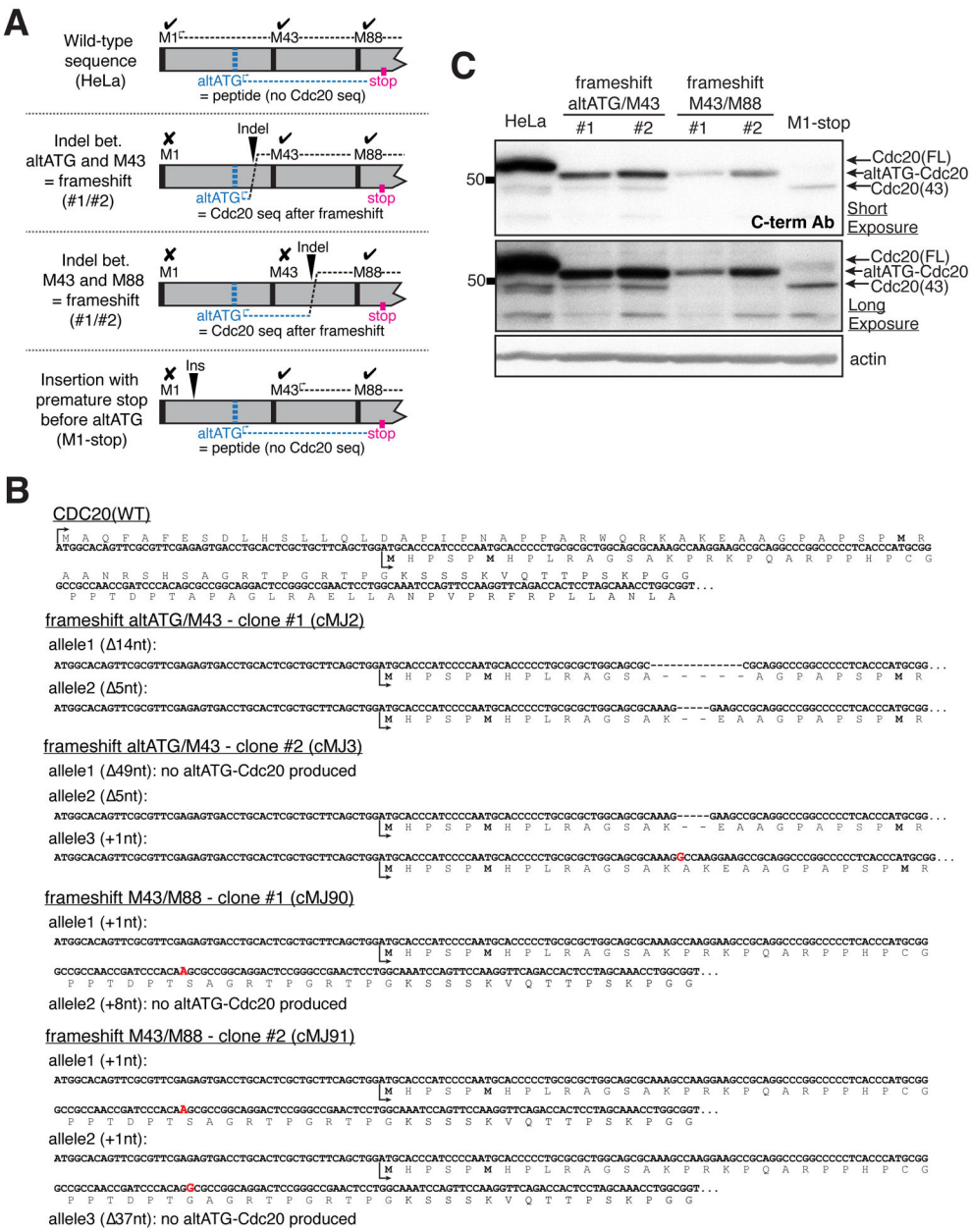

Extended Figure 3. Translation initiation at alternative out-of-frame start codons in HeLa cells. Related to Figure 1.

(**A**) Schematic illustrating the strategy to assess whether translation initiation occurs at the alternative out-of-frame start codons. Cdc20 protein indicated in black; altORF peptide indicated in blue and cyan. Cell lines with indel mutations after the alternative start codons at the endogenous locus in all *CDC20* alleles disrupt translation of the full-length Cdc20 protein. Some indel mutations resulted in a frame shift that would be predicted to connect the altORF peptide with amino acid sequences encoding downstream regions of Cdc20. If the altORF is translated, this would produce a chimeric protein (altATG-Cdc20) that is shorter than full-length Cdc20, but is detectable with antibodies against the Cdc20 C-terminus. In contrast, insertions upstream of the alternative out-of-frame start codons, such

as those in the M1-stop mutant, should only abrogated expression of the full-length Cdc20 protein without generating a chimeric altATG-Cdc20 protein. (**B**) Analysis of wild-type human *CDC20* nucleic acid sequence reveals two alternative out-of-frame start codons between Met1 and Met43. The amino acid sequence of the predicted alternative open reading frame (altORF) is indicated below the nucleic acid sequence, with the methionines bolded. Sequence information is shown for representative clones with indel mutations where at least one *CDC20* allele results in a frame shift that connects the altORF peptide with amino acid sequences encoding downstream regions of Cdc20. The DNA sequence of the genomic locus was determined by next-generation sequencing. Insertions are highlighted in red. When present, the amino acid sequence of the resulting altATG-Cdc20 peptide produced is shown. (**C**) Western blot showing mitotically-enriched control HeLa, M1-stop mutant, and representative clones with indel mutations where at least one *CDC20* allele resulted in a frame shift that connects the altORF peptide with amino acid sequences encoding downstream regions of Cdc20. Endogenous Cdc20 protein was detected using antibodies recognizing the C-terminus of human Cdc20 (aa 450-499). β-actin was used as loading control.

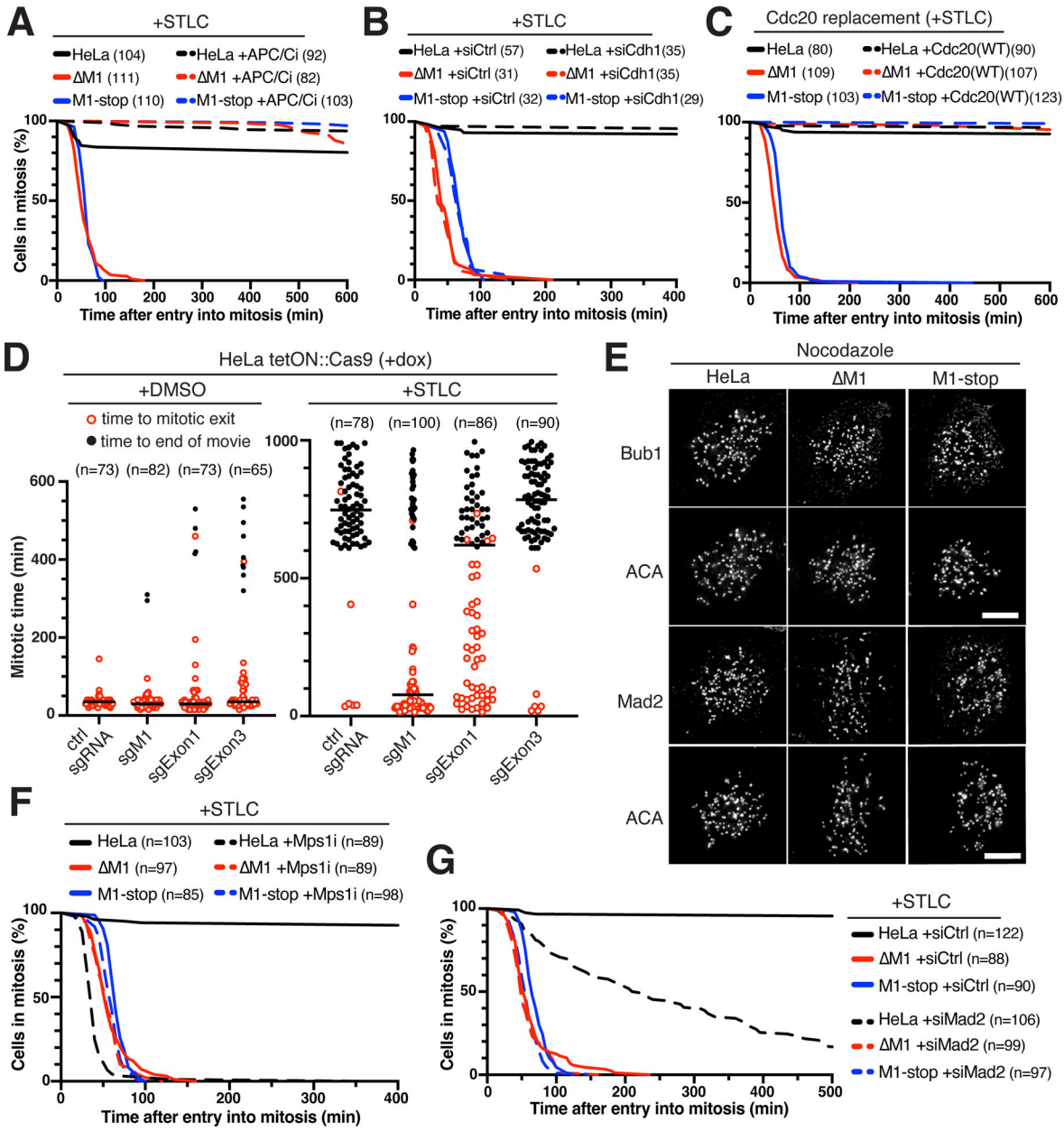

Extended Data Figure 4. Truncated Cdc20 isoforms are inefficient targets of the SAC and promote mitotic slippage. Related to Figure 2.

(**A**) Cumulative frequency distribution showing the fraction of mitotic cells over time post-mitotic entry for HeLa, ΔM1, and M1-stop cells treated with 10 μM STLC alone or in combination with the APC/C-inhibitor proTAME (12 μM). The total number of cells included in the analyses are indicated in brackets. (**B**) Cumulative frequency distribution as in (A) for HeLa, ΔM1, and M1-stop cells treated with 10 μM STLC and 100nM of either control siRNAs or Cdh1 siRNAs. (**C**) Cumulative frequency distribution as in (A) for HeLa, ΔM1, and M1-stop cells treated with 10 μM STLC and either expressing endogenous Cdc20 protein and treated with control siRNAs or upon Cdc20 replacement with ectopic wild-type *CDC20* cDNA. (**D**) Mitotic duration of individual HeLa cells

expressing doxycycline-inducible Cas9 and sgRNAs recognizing different regions within the *CDC20* gene. Unperturbed mitotic progression or mitotic arrest behavior were monitored upon treatment with DMSO or 10 μM STLC respectively. Cells entering mitosis in the first 350-400 min of time lapse experiments were included in the analyses. Open red circles indicate cells that exit mitosis. Closed black circles indicate cells that remained arrested in mitosis till the end of the time lapse. Bars correspond to the median. (**E**) Representative immunofluorescence images of Bub1 or Mad2 localization to kinetochores immuno-stained with anti-centromere antibodies (ACA). Images are maximum intensity projections of deconvolved Z-stacks of selected mitotic cells from control HeLa or mutant ΔM1 or M1-stop cell lines treated with nocodazole. Images were scaled individually to highlight kinetochore localization. Scale bar, 5 μm. (**F**) Cumulative frequency distribution as in (A) except for HeLa, ΔM1, and M1-stop cells treated with 10 μM STLC alone or in combination with the Mps1-inhibitor AZ3146 (4 μM). (**G**) Cumulative frequency distribution as in (A) except for HeLa, ΔM1, and M1-stop cells treated with 10 μM STLC and either control siRNAs or Mad2 siRNAs.

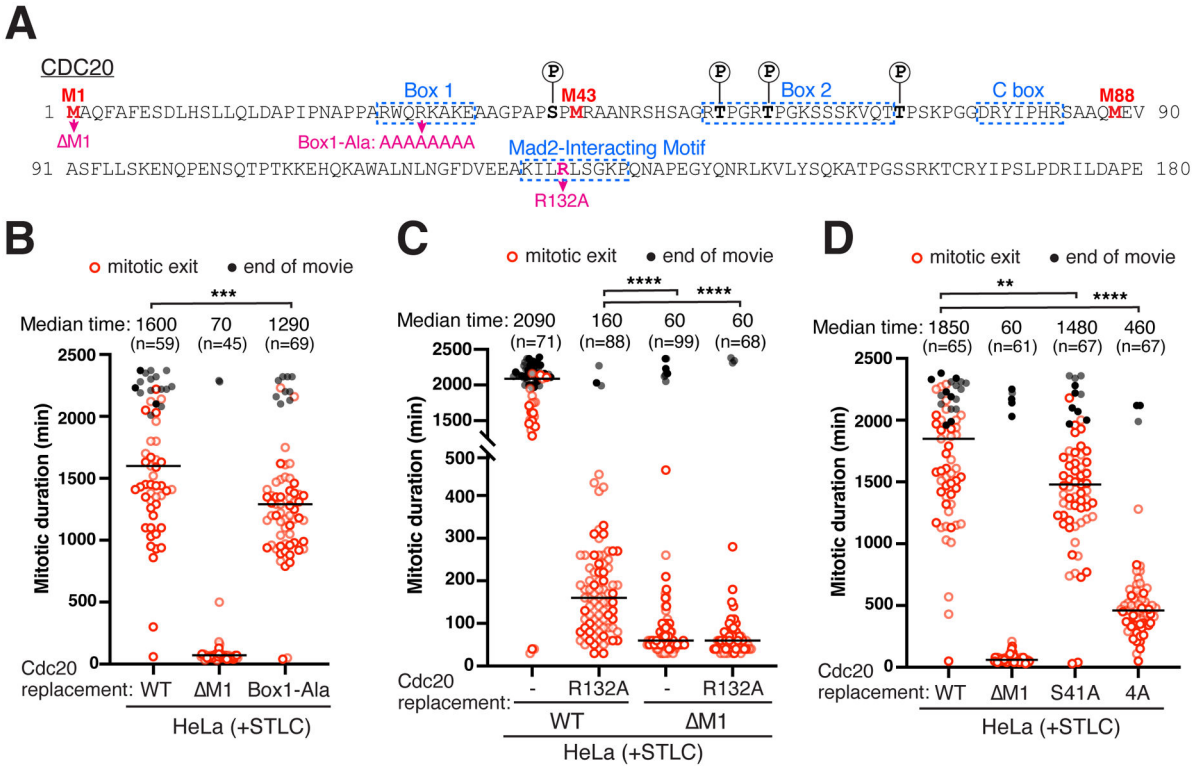

Extended Data Figure 5. Loss of amino acid sequences and protein interactions within the Cdc20 N-terminus results in SAC defect. Related to Figure 2.

(**A**) Protein sequence of the N-terminal region of human Cdc20 with conserved motifs and CDK phosphorylation sites indicated. Targeted mutations are shown in magenta. (**B**) Mitotic arrest duration in the presence of 10 μM STLC for individual HeLa cells in which the endogenous Cdc20 protein is replaced with either wild-type siRNA-resistant *CDC20* cDNA or ΔM1 or Box1-Ala mutant constructs. Cells entering mitosis in the first 450 min of time lapse experiments were included in analyses. Open red circles indicate cells that exit mitosis.

Closed black circles indicate cells that remained arrested in mitosis until the end of the time lapse. Bars correspond to median. Indicated are the median mitotic duration times across two experimental replicates, with replicates shaded-coded. The total number of cells analyzed is indicated. Statistics are from a Mann-Whitney Test (**p < 0.01, ***p < 0.001, ****p < 0.0001). (**C**) Mitotic arrest duration analysis as in (B) comparing the wild-type Cdc20 construct with R132A or ΔM1 alone or ΔM1 R132A double mutant constructs. (**D**) Mitotic arrest duration analysis as in (B) comparing the wild-type Cdc20 construct with either ΔM1, S41A, or 4A mutant constructs.

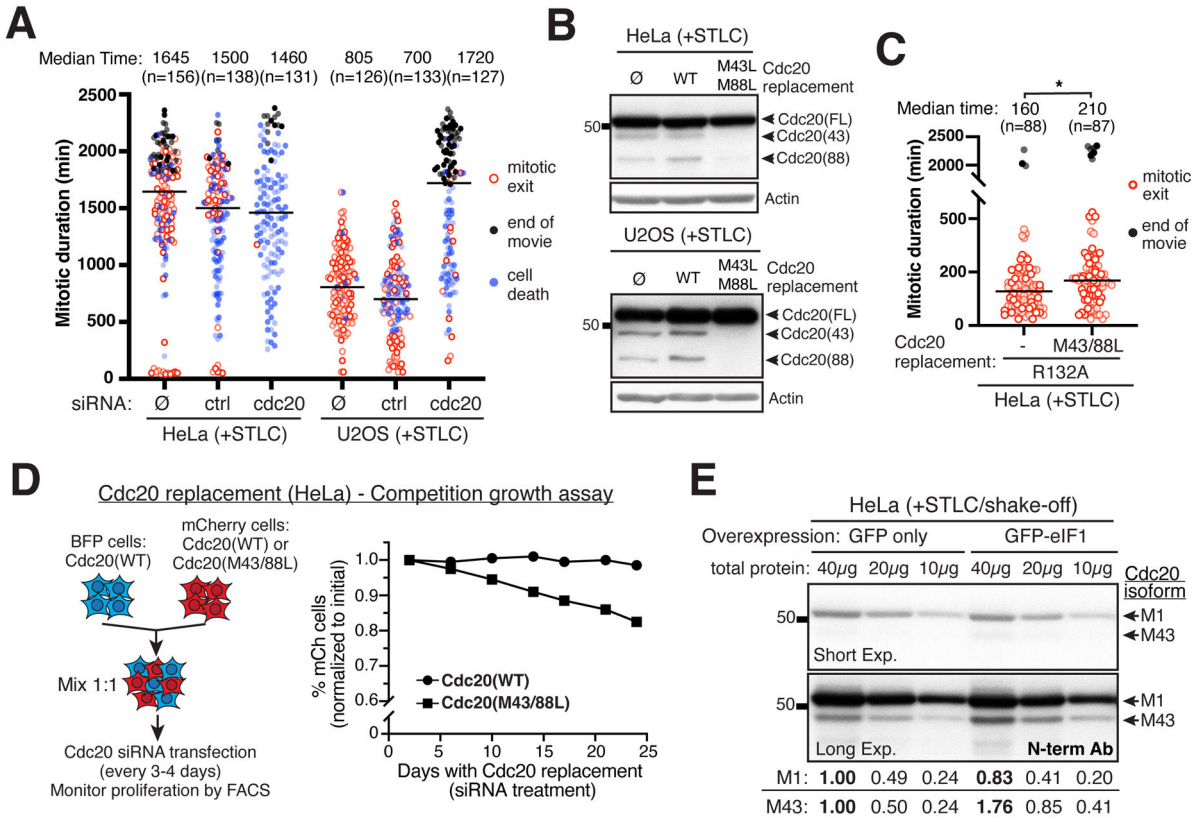

Extended Data Figure 6. Cdc20 translational isoforms modulate mitotic arrest duration. Related to Figure 3.

(**A**) Mitotic arrest duration of individual HeLa or U2OS cells treated with 10 μM STLC alone or with a combination of STLC and siRNA treatment (either control siRNAs or Cdc20 siRNAs). Cells entering mitosis in the first 600 min (HeLa) or 700 min (U2OS) of time lapse experiments were included in analyses. Open red circles indicate cells that exit mitosis. Closed black circles indicate cells that remained arrested in mitosis till the end of the time lapse. Blue circles indicate cells that die in mitosis. Bars correspond to median. Indicated are the median mitotic duration times across two experimental replicates, with replicates shaded-coded. The total number of cells analyzed is indicated. (**B**) Western blot of mitotically-enriched HeLa or U2OS cells expressing endogenous Cdc20 protein or upon Cdc20 replacement with either wild-type *CDC20* cDNA or a Cdc20 M43L M88L mutant construct. Cells were enriched in mitosis with 10 μM STLC for 18 hrs. Cdc20 protein was detected using antibodies recognizing the human Cdc20 C-terminus (aa 450-499). β-actin

was used as loading control. (**C**) Similar mitotic arrest duration analysis as in (A) except comparing HeLa cells in which the endogenous Cdc20 protein is replaced with siRNA-resistant *CDC20(R132A)* cDNA or a *CDC20(M43L M88L R132A)* mutant construct. NOTE: data for the *CDC20(R132A)* mutant is duplicated from Extended Fig. 5C. Statistics are from Mann-Whitney Test (*$p < 0.05$). (**D**) Competitive proliferation assay with long-term conditional Cdc20 replacement. Left, schematic of competitive proliferation assay. BFP-expressing HeLa cells with an ectopic siRNA-resistant *CDC20(WT)* construct were mixed 1:1 with mCherry-expressing HeLa cells with similar *CDC20(WT)* or *CDC20(M43L M88L)* constructs. Endogenous Cdc20 protein was depleted by siRNA transfection every 3-4 days for 24 days. Right, graph monitoring proliferation by flow cytometry analysis. The percentage of mCherry-positive cells at the indicated timepoint was quantified and normalized to the initial levels determined two days after the first siRNA transfection. (**E**) Western blot of single-thymidine synchronized HeLa cells expressing GFP alone or GFP-eIF1 post-release into medium with STLC for 16 hrs. Cdc20 isoform levels in serial diluted lysates were quantified for the full-length and M43 isoforms from short exposure and long exposure images respectively with antibodies recognizing the two Cdc20 isoforms. The levels in the undiluted HeLa sample expressing GFP alone (40 μg) were set to 1.

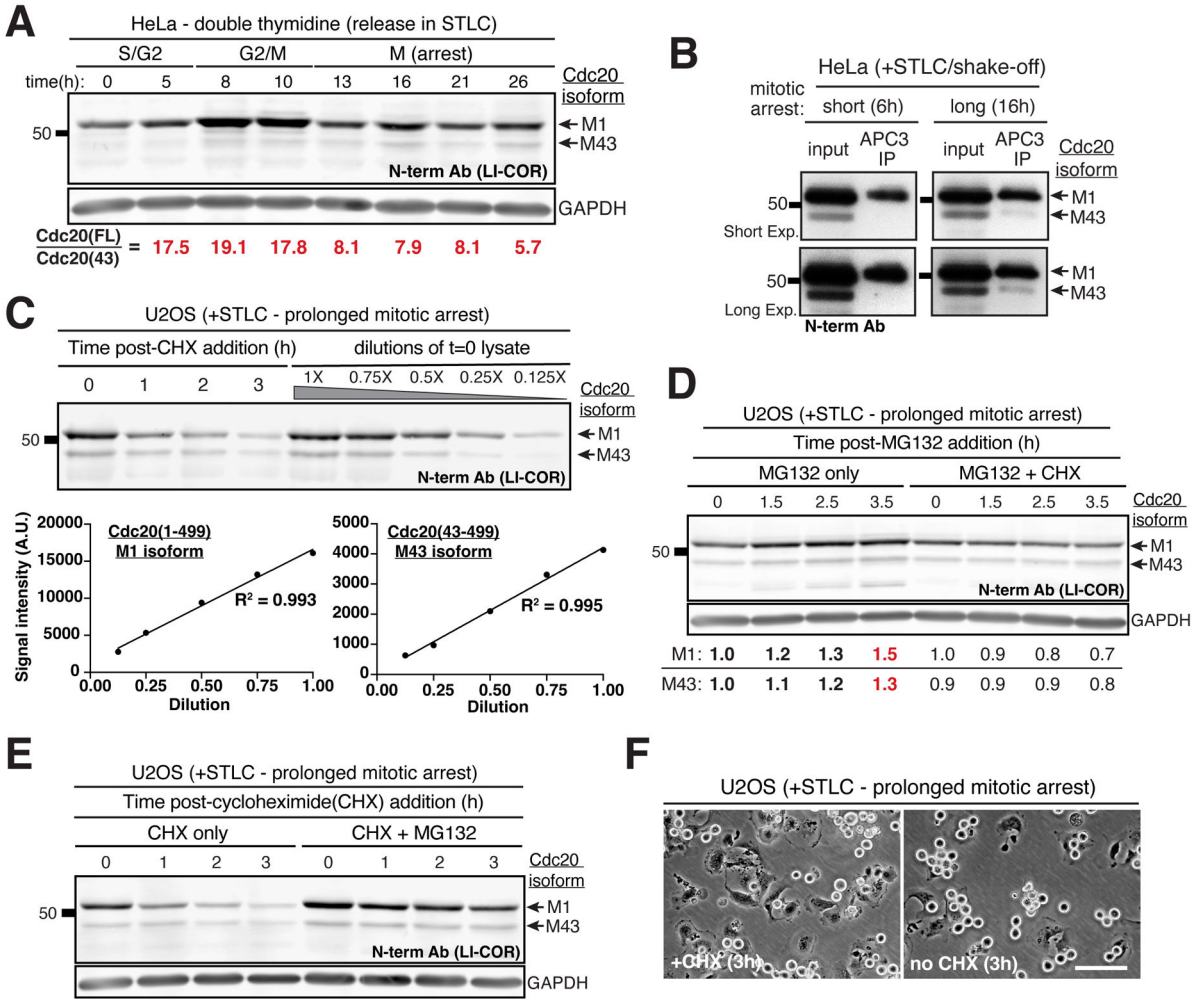

Extended Data Figure 7. Cdc20 isoform levels change during a prolonged mitotic arrest to promote mitotic slippage. Related to Figure 4.

(**A**) Western blot showing HeLa cells that were synchronized using double-thymidine block and harvested at different time points post-release with STLC treatment to induce a prolonged mitotic arrest. Cdc20 isoform levels were determined with antibodies recognizing the full-length and M43 isoforms. GAPDH was used as loading control. The ratio of full-length:M43 isoforms was quantified at the indicated time points using a LI-COR system. (**B**) Western blot of immunoprecipitated APC/C from mitotically-arrested HeLa cells harvested by shake-off after treatment with STLC for 6 hrs (short mitotic arrest) or 16 hrs (long mitotic arrest). APC/C-bound Cdc20 proteins were detected using antibodies against the N-terminus of Cdc20 antibodies recognizing the full-length and M43 isoforms. (**C**) Western blot showing mitotically-arrested U2OS cells harvested at various time points after addition of 50 μg/ml cycloheximide to inhibit new protein synthesis. Serial dilutions of the initial untreated cells were quantified for the full-length and M43 isoforms using a LI-COR system to determine the linear range of the N-terminal Cdc20 antibody recognizing the two Cdc20 isoforms. (**D**) Western blot as in (C) showing U2OS cells treated with 10 μM MG-132 alone to assess new protein synthesis or together with 50 μg/ml cycloheximide to inhibit new protein synthesis. Cdc20 isoform levels were quantified for the full-length

and M43 isoform using a LI-COR system and GAPDH was used as loading control. The levels in the initial MG-132 only cells were set to 1. (**E**) Western blot as in (C) showing U2OS cells treated with 50 μg/ml cycloheximide alone or together with 10 μM MG-132 to inhibit proteosome-mediated degradation. (**F**) Representative phase contrast images of mitotically-arrested U2OS cells at 3 hrs post-cycloheximide addition or the corresponding untreated cells. NOTE: Larger field view of images in Fig. 4D. Scale bar, 100 μm.

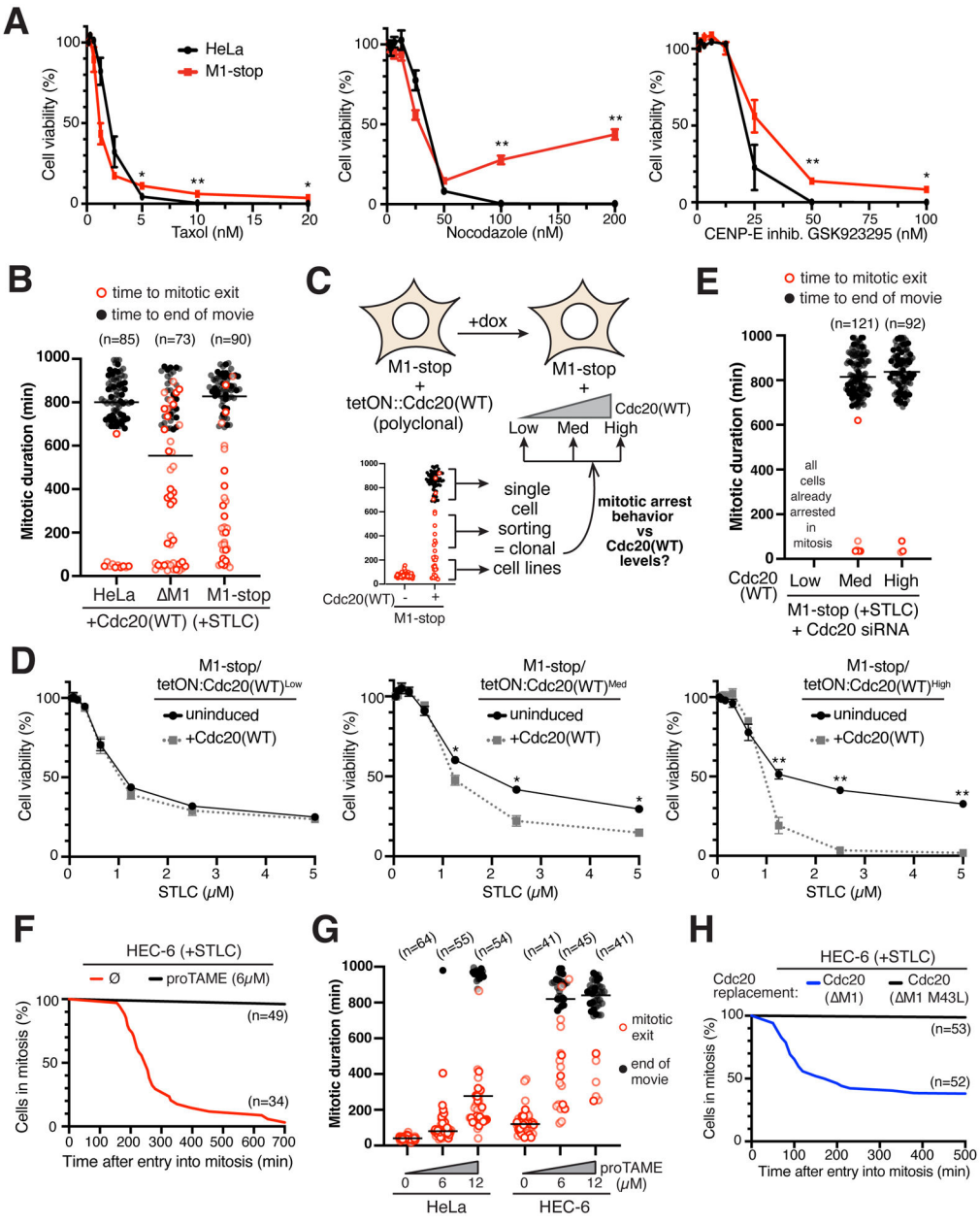

Extended Data Figure 8. Cdc20 translational isoform levels alter cancer cell anti-mitotic drug sensitivity. Related to Figure 5.

(**A**) Sensitivity of HeLa or M1-stop cells to increasing concentrations of Taxol, Nocodazole, or the CENP-E inhibitor GSK923295. Cell viability was determined by MTT assay in

triplicate following 72 h drug treatment. Data are mean ± s.e.m from three (Nocodazole) or four (Taxol, GSK923295) experimental replicates. Statistics from Student's two-sample t-Test with two-tailed distribution comparing HeLa and M1-stop cell viabilities per drug concentration (*p < 0.05, **p < 0.01). (**B**) Mitotic arrest duration in the presence of 10 μM STLC for individual HeLa, ΔM1, or M1-stop cells expressing the wild-type *CDC20* cDNA. Open red circles indicate cells that exit mitosis. Closed black circles indicate cells that remained arrested in mitosis till the end of the time lapse. Bars correspond to the median across two experimental replicates, with replicates shaded-coded. The total number of cells analyzed is indicated. (**C**) Schematic illustrating the approach to isolate clonal cell lines from the polyclonal M1-stop mutant expressing the doxycycline-inducible wild-type *CDC20* construct. Multiple clones were analyzed to assess the correlation between the mitotic arrest behavior of a given clone and the expression level of the integrated doxycycline-inducible *CDC20* construct (see text for details). (**D**) Similar sensitivity assay as in (A) except for STLC for representative clones of M1-stop mutant with low, medium, or high expression of the doxycycline-inducible wild-type *CDC20* construct without induction or induced with 20 ng/ml doxycycline. Data are mean ± s.e.m from three experimental replicates. Statistics from Student's two-sample t-Test with two-tailed distribution comparing the uninduced and induced cell viabilities per drug concentration (*p < 0.05, **p < 0.01). (**E**) Similar mitotic arrest duration as in (B) except for representative clones of M1-stop mutant with low, medium, or high expression of the doxycycline-inducible wild-type *CDC20* construct. Cells were treated with Cdc20 siRNAs to deplete endogenous truncated Cdc20 isoforms. Low Cdc20 expression from the inducible *CDC20* construct fails to support mitotic progression even before addition of STLC. (**F**) Cumulative frequency distribution for the fraction of cells in mitosis at the indicated time after entry into mitosis (mitotic arrest duration) for HEC-6 cells treated with 10 μM STLC alone or together with 6 μM proTAME. The total number of cells analyzed across two experimental replicates is indicated. (**G**) Mitotic duration in the presence of increasing concentrations of proTAME for individual HeLa or HEC-6 cells. Symbols are as described in (B). Indicated are the median mitotic duration times across two experimental replicates, with the total number of cells analyzed and replicates shaded-coded. (**H**) Cumulative frequency distribution as in (F) for HEC-6 cells that had the endogenous Cdc20 protein replaced with either *CDC20(ΔM1)* or *CDC20(ΔM1 M43L)* mutant constructs.

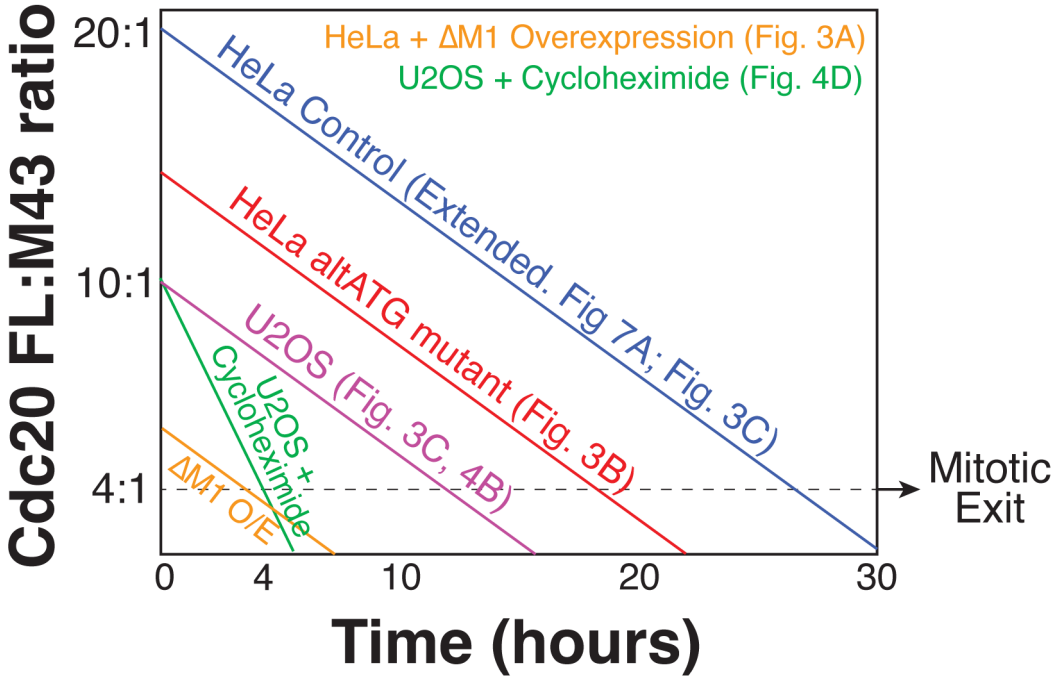

Extended Data Figure 9. Differential turnover of Cdc20 isoforms creates a mitotic arrest timer.

Diagram showing changing Cdc20 isoform ratios across the indicated conditions inferred from the data in the referenced experiments. We propose the changing levels of the Cdc20 isoforms in arrested cells occurs due to differential protein turnover creating a molecular timer to directly control the mitotic arrest duration. When the short M43 isoform reaches a ratio such that it comprises approximately one quarter of the total Cdc20 protein, it will be able to activate a sufficient portion of the APC/C to trigger mitotic exit even in the presence of continued SAC activation. The graph highlights multiple experiments conducted in this paper to alter Cdc20 isoform ratios or prevent new protein synthesis.

Supplementary Material

Refer to Web version on PubMed Central for supplementary material.

Acknowledgements

The authors thank Kuan-Chung Su for his support, insights, and guidance, Kara McKinley for initial observations, Eric Spooner for assistance with the mass spectrometry analysis, George Bell for analyzing the altORF conservation, and Angelika Amon, Dave Bartel, and members of the Cheeseman lab for their critical input and suggestions. This work was supported by grants to IMC from the NIH/National Institute of General Medical Sciences (R35GM126930), National Science Foundation (2029868), the Gordon and Betty Moore Foundation, the American Cancer Society (Theory Lab Collaborative Grant (TLC-20-117-01-TLC)), and a Hope Funds for Cancer Research fellowship (HFCR-18-03-02) to MJT.

Data Availability

The data that support the findings of this study are available from the corresponding author upon reasonable request.

References

1. Musacchio A The Molecular Biology of Spindle Assembly Checkpoint Signaling Dynamics. Curr Biol 25, R1002–1018 (2015). 10.1016/j.cub.2015.08.051 [PubMed: 26485365]
2. Lara-Gonzalez P, Pines J & Desai A Spindle assembly checkpoint activation and silencing at kinetochores. Semin Cell Dev Biol 117, 86–98 (2021). 10.1016/j.semcdb.2021.06.009 [PubMed: 34210579]
3. Sivakumar S & Gorbsky GJ Spatiotemporal regulation of the anaphase-promoting complex in mitosis. Nat Rev Mol Cell Biol 16, 82–94 (2015). 10.1038/nrm3934 [PubMed: 25604195]
4. Eichhorn JM, Sakurikar N, Alford SE, Chu R & Chambers TC Critical role of anti-apoptotic Bcl-2 protein phosphorylation in mitotic death. Cell Death Dis 4, e834 (2013). 10.1038/cddis.2013.360 [PubMed: 24091677]
5. Li M, York JP & Zhang P Loss of Cdc20 causes a securin-dependent metaphase arrest in two-cell mouse embryos. Mol Cell Biol 27, 3481–3488 (2007). 10.1128/mcb.02088-06 [PubMed: 17325031]
6. Lim HH, Goh PY & Surana U Cdc20 is essential for the cyclosome-mediated proteolysis of both Pds1 and Clb2 during M phase in budding yeast. Curr Biol 8, 231–234 (1998). 10.1016/s0960-9822(98)70088-0 [PubMed: 9501986]
7. McKinley KL & Cheeseman IM Large-Scale Analysis of CRISPR/Cas9 Cell-Cycle Knockouts Reveals the Diversity of p53-Dependent Responses to Cell-Cycle Defects. Dev Cell 40, 405–420 e402 (2017). 10.1016/j.devcel.2017.01.012 [PubMed: 28216383]
8. Consortium, G. T. Human genomics. The Genotype-Tissue Expression (GTEx) pilot analysis: multitissue gene regulation in humans. Science 348, 648–660 (2015). 10.1126/science.1262110 [PubMed: 25954001]
9. Hartwell LH, Mortimer RK, Culotti J & Culotti M Genetic Control of the Cell Division Cycle in Yeast: V. Genetic Analysis of cdc Mutants. Genetics 74, 267–286 (1973). [PubMed: 17248617]
10. Tsherniak A et al. Defining a Cancer Dependency Map. Cell 170, 564–576 e516 (2017). 10.1016/j.cell.2017.06.010 [PubMed: 28753430]
11. Smith LM, Kelleher NL & Consortium for Top Down, P. Proteoform: a single term describing protein complexity. Nat Methods 10, 186–187 (2013). 10.1038/nmeth.2369 [PubMed: 23443629]
12. Hinnebusch AG The scanning mechanism of eukaryotic translation initiation. Annu Rev Biochem 83, 779–812 (2014). 10.1146/annurev-biochem-060713-035802 [PubMed: 24499181]
13. Kozak M. Initiation of translation in prokaryotes and eukaryotes. Gene 234, 187–208 (1999). 10.1016/s0378-1119(99)00210-3 [PubMed: 10395892]
14. Kozak M. Pushing the limits of the scanning mechanism for initiation of translation. Gene 299, 1–34 (2002). 10.1016/s0378-1119(02)01056-9 [PubMed: 12459250]
15. Lischetti T, Zhang G, Sedgwick GG, Bolanos-Garcia VM & Nilsson J The internal Cdc20 binding site in BubR1 facilitates both spindle assembly checkpoint signalling and silencing. Nat Commun 5, 5563 (2014). 10.1038/ncomms6563 [PubMed: 25482201]
16. Di Fiore B et al. The ABBA motif binds APC/C activators and is shared by APC/C substrates and regulators. Dev Cell 32, 358–372 (2015). 10.1016/j.devcel.2015.01.003 [PubMed: 25669885]
17. Izawa D & Pines J The mitotic checkpoint complex binds a second CDC20 to inhibit active APC/C. Nature 517, 631–634 (2015). 10.1038/nature13911 [PubMed: 25383541]
18. Nilsson J, Yekezare M, Minshull J & Pines J The APC/C maintains the spindle assembly checkpoint by targeting Cdc20 for destruction. Nat Cell Biol 10, 1411–1420 (2008). 10.1038/ncb1799 [PubMed: 18997788]
19. Zhang S et al. Molecular mechanism of APC/C activation by mitotic phosphorylation. Nature 533, 260–264 (2016). 10.1038/nature17973 [PubMed: 27120157]
20. Kimata Y, Baxter JE, Fry AM & Yamano H A role for the Fizzy/Cdc20 family of proteins in activation of the APC/C distinct from substrate recruitment. Mol Cell 32, 576–583 (2008). 10.1016/j.molcel.2008.09.023 [PubMed: 19026787]
21. Ji Z, Gao H, Jia L, Li B & Yu H A sequential multi-target Mps1 phosphorylation cascade promotes spindle checkpoint signaling. Elife 6 (2017). 10.7554/eLife.22513

22. Piano V et al. CDC20 assists its catalytic incorporation in the mitotic checkpoint complex. Science 371, 67–71 (2021). 10.1126/science.abc1152 [PubMed: 33384373]
23. Lara-Gonzalez P, Kim T, Oegema K, Corbett K & Desai A A tripartite mechanism catalyzes Mad2-Cdc20 assembly at unattached kinetochores. Science 371, 64–67 (2021). 10.1126/science.abc1424 [PubMed: 33384372]
24. Zeng X et al. Pharmacologic inhibition of the anaphase-promoting complex induces a spindle checkpoint-dependent mitotic arrest in the absence of spindle damage. Cancer Cell 18, 382–395 (2010). 10.1016/j.ccr.2010.08.010 [PubMed: 20951947]
25. Visintin R, Prinz S & Amon A CDC20 and CDH1: a family of substrate-specific activators of APC-dependent proteolysis. Science 278, 460–463 (1997). 10.1126/science.278.5337.460 [PubMed: 9334304]
26. Yudkovsky Y, Shteinberg M, Listovsky T, Brandeis M & Hershko A Phosphorylation of Cdc20/fizzy negatively regulates the mammalian cyclosome/APC in the mitotic checkpoint. Biochem Biophys Res Commun 271, 299–304 (2000). 10.1006/bbrc.2000.2622 [PubMed: 10799291]
27. Labit H et al. Dephosphorylation of Cdc20 is required for its C-box-dependent activation of the APC/C. EMBO J 31, 3351–3362 (2012). 10.1038/emboj.2012.168 [PubMed: 22713866]
28. Hein JB, Hertz EPT, Garvanska DH, Kruse T & Nilsson J Distinct kinetics of serine and threonine dephosphorylation are essential for mitosis. Nat Cell Biol 19, 1433–1440 (2017). 10.1038/ncb3634 [PubMed: 29084198]
29. Orth JD et al. Quantitative live imaging of cancer and normal cells treated with Kinesin-5 inhibitors indicates significant differences in phenotypic responses and cell fate. Mol Cancer Ther 7, 3480–3489 (2008). 10.1158/1535-7163.Mct-08-0684 [PubMed: 18974392]
30. Varetti G, Guida C, Santaguida S, Chiroli E & Musacchio A Homeostatic control of mitotic arrest. Mol Cell 44, 710–720 (2011). 10.1016/j.molcel.2011.11.014 [PubMed: 22152475]
31. Lok TM et al. Mitotic slippage is determined by p31(comet) and the weakening of the spindle-assembly checkpoint. Oncogene 39, 2819–2834 (2020). 10.1038/s41388-020-1187-6 [PubMed: 32029899]
32. Gascoigne KE & Taylor SS Cancer cells display profound intra- and interline variation following prolonged exposure to antimitotic drugs. Cancer Cell 14, 111–122 (2008). 10.1016/j.ccr.2008.07.002 [PubMed: 18656424]
33. Pestova TV & Kolupaeva VG The roles of individual eukaryotic translation initiation factors in ribosomal scanning and initiation codon selection. Genes Dev 16, 2906–2922 (2002). 10.1101/gad.1020902 [PubMed: 12435632]
34. Ivanov IP, Loughran G, Sachs MS & Atkins JF Initiation context modulates autoregulation of eukaryotic translation initiation factor 1 (eIF1). Proc Natl Acad Sci U S A 107, 18056–18060 (2010). 10.1073/pnas.1009269107 [PubMed: 20921384]
35. Partscht P, Simon A, Chen NP, Erhardt S & Schiebel E The HIPK2/CDC14B-MeCP2 axis enhances the spindle assembly checkpoint block by promoting cyclin B translation. Sci Adv 9, eadd6982 (2023). 10.1126/sciadv.add6982 [PubMed: 36662865]
36. Sloss O, Topham C, Diez M & Taylor S Mcl-1 dynamics influence mitotic slippage and death in mitosis. Oncotarget 7, 5176–5192 (2016). 10.18632/oncotarget.6894 [PubMed: 26769847]
37. Brito DA & Rieder CL Mitotic checkpoint slippage in humans occurs via cyclin B destruction in the presence of an active checkpoint. Curr Biol 16, 1194–1200 (2006). 10.1016/j.cub.2006.04.043 [PubMed: 16782009]
38. Jordan MA & Wilson L Microtubules as a target for anticancer drugs. Nat Rev Cancer 4, 253–265 (2004). 10.1038/nrc1317 [PubMed: 15057285]
39. Weaver BA How Taxol/paclitaxel kills cancer cells. Mol Biol Cell 25, 2677–2681 (2014). 10.1091/mbc.E14-04-0916 [PubMed: 25213191]
40. Huang HC, Shi J, Orth JD & Mitchison TJ Evidence that mitotic exit is a better cancer therapeutic target than spindle assembly. Cancer Cell 16, 347–358 (2009). 10.1016/j.ccr.2009.08.020 [PubMed: 19800579]
41. Cheng B & Crasta K Consequences of mitotic slippage for antimicrotubule drug therapy. Endocr Relat Cancer 24, T97–T106 (2017). 10.1530/erc-17-0147 [PubMed: 28684541]

42. Kochetov AV Alternative translation start sites and hidden coding potential of eukaryotic mRNAs. Bioessays 30, 683–691 (2008). 10.1002/bies.20771 [PubMed: 18536038]
43. Lee S et al. Global mapping of translation initiation sites in mammalian cells at single-nucleotide resolution. Proc Natl Acad Sci U S A 109, E2424–2432 (2012). 10.1073/pnas.1207846109 [PubMed: 22927429]
44. Van Damme P, Gawron D, Van Criekinge W & Menschaert G N-terminal proteomics and ribosome profiling provide a comprehensive view of the alternative translation initiation landscape in mice and men. Mol Cell Proteomics 13, 1245–1261 (2014). 10.1074/mcp.M113.036442 [PubMed: 24623590]
45. Chen J et al. Pervasive functional translation of noncanonical human open reading frames. Science 367, 1140–1146 (2020). 10.1126/science.aay0262 [PubMed: 32139545]
46. Cornelis S et al. Identification and characterization of a novel cell cycle-regulated internal ribosome entry site. Mol Cell 5, 597–605 (2000). 10.1016/s1097-2765(00)80239-7 [PubMed: 10882096]
47. Cong L et al. Multiplex genome engineering using CRISPR/Cas systems. Science 339, 819–823 (2013). 10.1126/science.1231143 [PubMed: 23287718]
48. Morgenstern JP & Land H Advanced mammalian gene transfer: high titre retroviral vectors with multiple drug selection markers and a complementary helper-free packaging cell line. Nucleic Acids Res 18, 3587–3596 (1990). 10.1093/nar/18.12.3587 [PubMed: 2194165]
49. Qian K et al. A simple and efficient system for regulating gene expression in human pluripotent stem cells and derivatives. Stem Cells 32, 1230–1238 (2014). 10.1002/stem.1653 [PubMed: 24497442]
50. Sliedrecht T, Zhang C, Shokat KM & Kops GJ Chemical genetic inhibition of Mps1 in stable human cell lines reveals novel aspects of Mps1 function in mitosis. PLoS One 5, e10251 (2010). 10.1371/journal.pone.0010251 [PubMed: 20422024]
51. Berg S et al. ilastik: interactive machine learning for (bio)image analysis. Nat Methods 16, 1226–1232 (2019). 10.1038/s41592-019-0582-9 [PubMed: 31570887]
52. McQuin C et al. CellProfiler 3.0: Next-generation image processing for biology. PLoS Biol 16, e2005970 (2018). 10.1371/journal.pbio.2005970 [PubMed: 29969450]
53. Papadopoulos JS & Agarwala R COBALT: constraint-based alignment tool for multiple protein sequences. Bioinformatics 23, 1073–1079 (2007). 10.1093/bioinformatics/btm076 [PubMed: 17332019]
54. Yates AD et al. Ensembl 2020. Nucleic Acids Res 48, D682–D688 (2020). 10.1093/nar/gkz966 [PubMed: 31691826]
55. Cheeseman IM & Desai A A combined approach for the localization and tandem affinity purification of protein complexes from metazoans. Sci STKE 2005, pl1 (2005). 10.1126/stke.2662005pl1 [PubMed: 15644491]

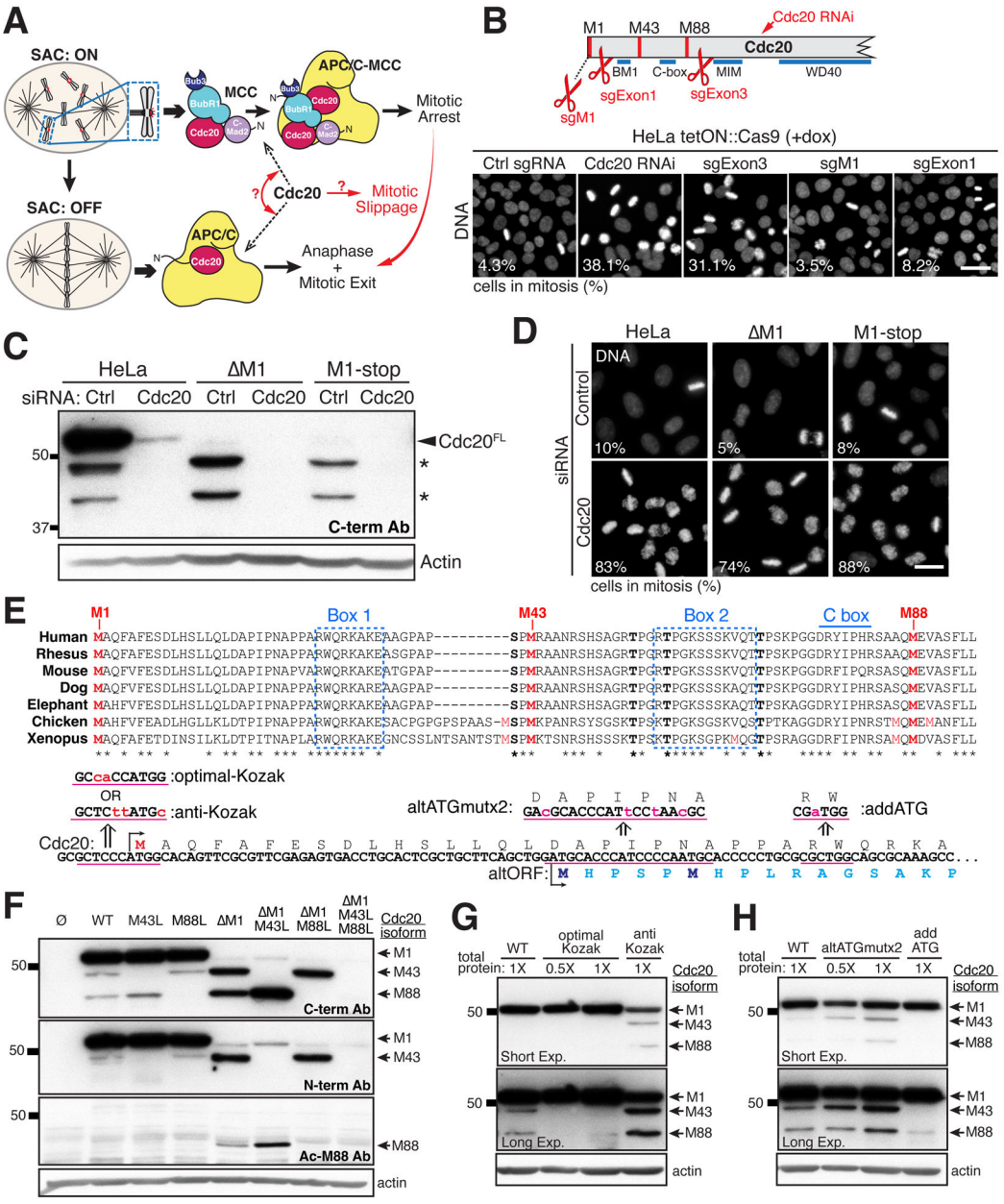

Figure 1. Human cells express alternative Cdc20 translational isoforms

(**A**) Diagram highlighting the opposing roles of Cdc20 as the key target of the SAC and an essential APC/C coactivator required for mitotic progression (based on [1]). (**B**) Top, Cdc20 open reading frame indicating the targeting of Cdc20 RNAi and sgRNAs. Bottom, representative images of DNA staining (Hoechst) showing the mitotic arrest behavior of HeLa cells after the indicated treatments. Numbers are average percent of cells in mitosis from two experimental replicates. Scale bar, 40 μm. (**C**) Western blot showing endogenous Cdc20 protein in HeLa, ΔM1, or M1-stop cells treated with control or Cdc20 siRNAs. (**D**) Representative images of DNA staining (Hoechst) showing the mitotic arrest behavior of HeLa, ΔM1, and M1-stop cells with control or Cdc20 siRNAs. Numbers are percent of cells in mitosis. Scale bar, 20 μm. (**E**) Top, protein alignment of Cdc20 N-terminal region

from the indicated species. Conserved amino acids indicated with asterisks. Bottom, human *CDC20* nucleic acid sequence reveals out-of-frame start codons between Met1 and Met43 that result in an alternative open reading frame (altORF; cyan). Targeted mutations are indicated. (**F**) Western blot assessing translation initiation at Met1, Met43, and/or Met88 start codons. Wild-type or the indicated Cdc20 mutants were expressed ectopically in mitotically-enriched M1-stop cells depleted of endogenous Cdc20 protein using RNAi and probed with the indicated antibodies. (**G**) Western blot of *CDC20* constructs with mutations altering the translation-initiation context of Met1 to the consensus Kozak sequence (optimal-Kozak) or an anti-Kozak sequence. Constructs were expressed in mitotically-enriched M1-stop cells depleted of endogenous Cdc20 and probed with antibodies against Cdc20 C-terminus. (**H**) Western blot as in (G) showing *CDC20* constructs with silent mutations to disrupt the out-of-frame start codons (altATGmutx2) or introduce an additional out-of-frame start codon (addATG).

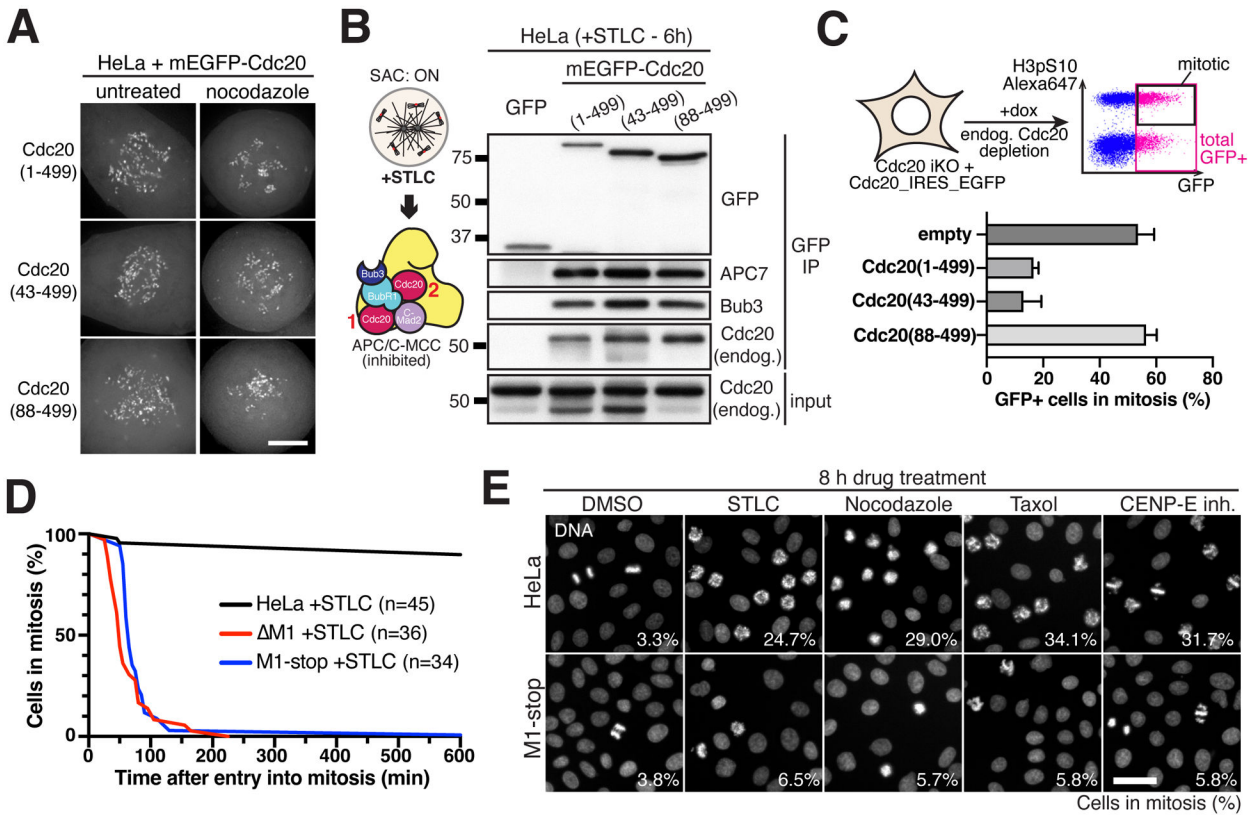

Figure 2. Truncated Cdc20 proteoforms are inefficient targets of the SAC.

(**A**) Representative live-cell fluorescence images of HeLa cells expressing the indicated mEGFP-Cdc20 fusions induced with 5 ng/ml doxycycline. Maximum intensity projections of deconvolved Z-stacks scaled individually to highlight kinetochore localization. Scale bar, 5 μm. (**B**) Western blot following GFP immunoprecipitation of mEGFP-Cdc20 fusions expressed in mitotically-enriched HeLa cells probed with the indicated antibodies. (**C**) Flow cytometry analysis of mitotic cells based on phospho-histone H3 staining in GFP-positive cells. Data are mean ± s.d. from two experimental replicates. Polyclonal cells constitutively-expressing the indicated constructs were depleted of endogenous Cdc20 using the sgExon3 guide. (**D**) Cumulative fraction of cells in mitosis at the indicated time after mitotic entry (mitotic arrest duration) for HeLa, ΔM1, and M1-stop cells treated with STLC. The total number of cells analyzed is indicated. (**E**) Representative images of DNA staining (Hoechst) showing the mitotic arrest behavior of HeLa or M1-stop cells treated with the indicated anti-mitotic drugs. Numbers are average percent of cells in mitosis from two experimental replicates. Scale bar, 40 μm.

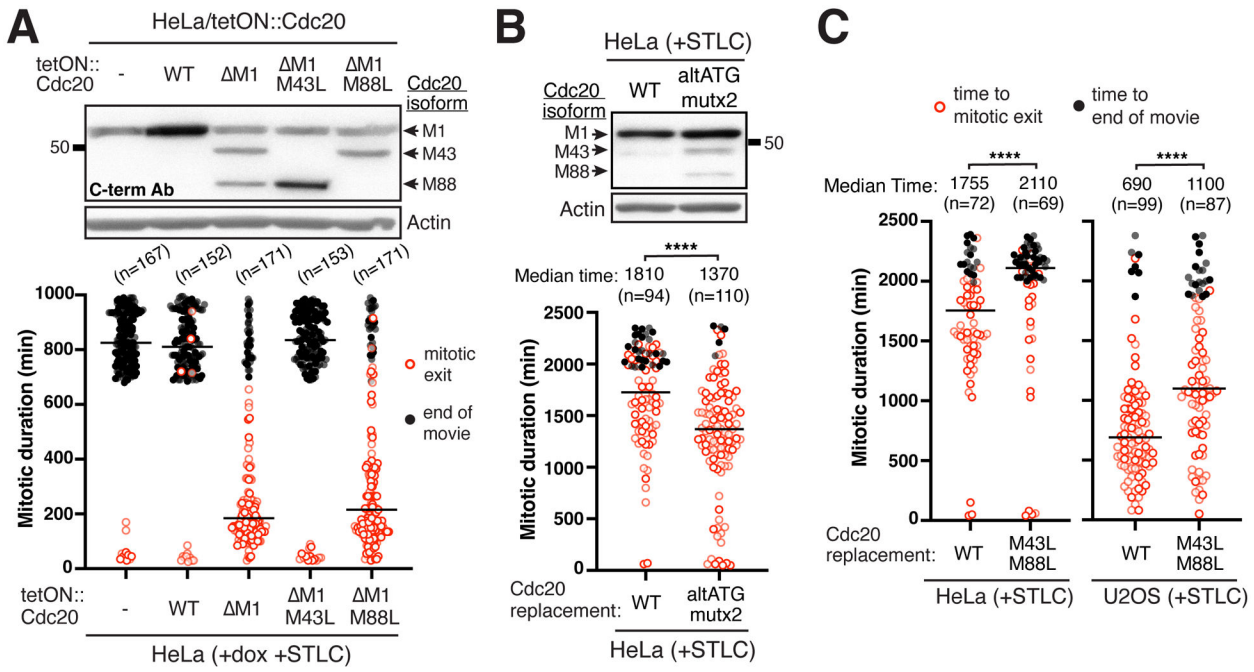

Figure 3. Cdc20 proteoform levels modulate mitotic arrest duration.

(**A**) Top, Western blot showing Cdc20 proteoforms present in HeLa cells alone or treated with 50 ng/ml doxycycline to induce expression of the indicated *CDC20* constructs. Bottom, mitotic arrest duration of individual HeLa cells treated with STLC alone or together with 50 ng/ml doxycycline to induce expression of the indicated *CDC20* constructs. Shown are cells entering mitosis in the first 325 min that either exit mitosis (open circles) or remain arrested for the duration of the analysis (black circles). Bars correspond to median across two experimental replicates, with replicates shaded-coded. The total number of cells analyzed is indicated. (**B**) Top, Western blot as in (A) showing mitotically-enriched HeLa cells in which the endogenous Cdc20 protein is replaced with either wild-type siRNA-resistant *CDC20* cDNA or a mutant disrupting altORF start codons (altATGmutx2). Bottom, mitotic arrest duration analysis as in (A) comparing the indicated *CDC20* constructs. Cells entering mitosis in the first 450 min were included in analyses. (**C**) Mitotic arrest duration analysis as in (A,B) for individual HeLa or U2OS cells with Cdc20 replacements with either wild-type *CDC20* cDNA or a Cdc20 M43L M88L mutant construct. Cells entering mitosis in the first 450 min (HeLa) or 600 min (U2OS) were included in analyses. Statistics in (B,C) from Mann-Whitney Test (****$p < 0.0001$).

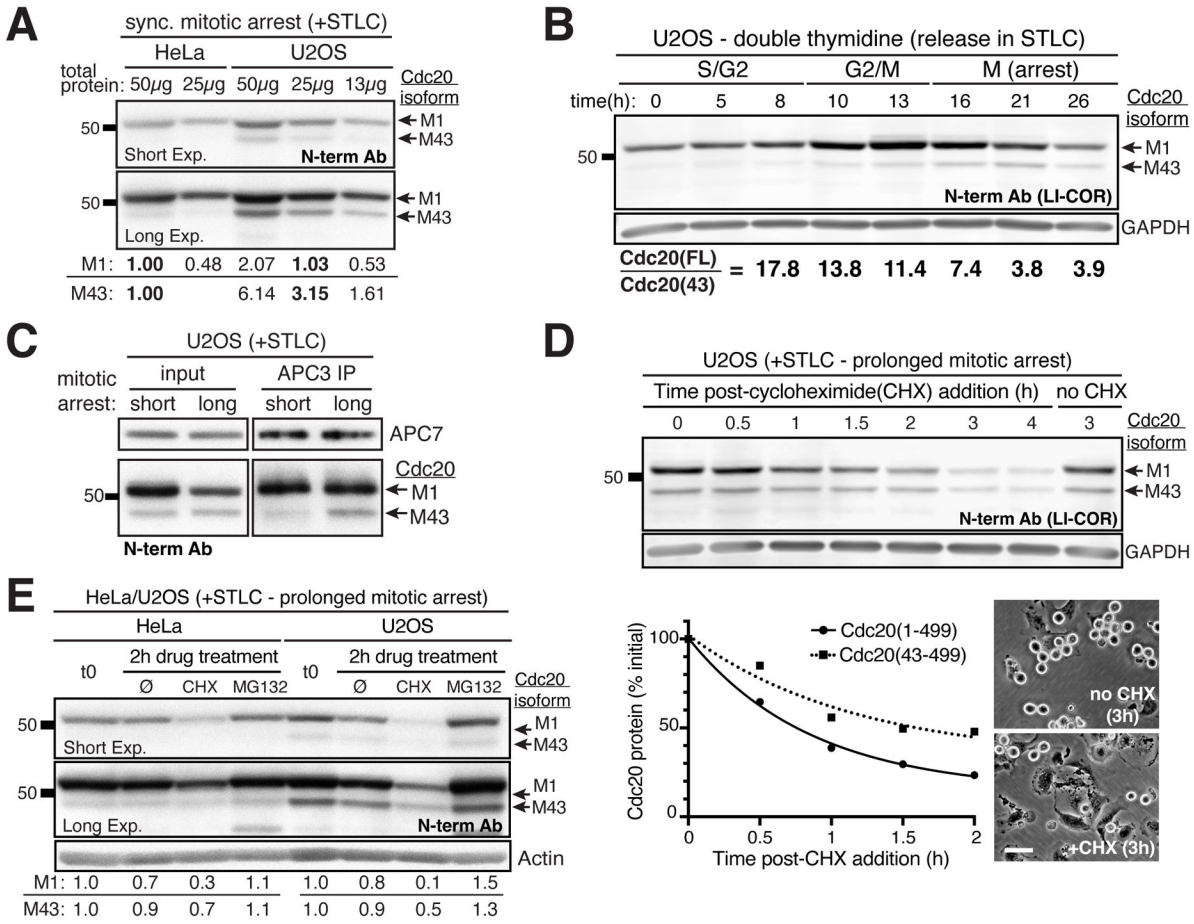

Figure 4. Cdc20 proteoform levels change during a mitotic arrest.

(**A**) Western blot showing HeLa or U2OS cells synchronized using double-thymidine block and harvested 21 hrs post-release with STLC treatment to induce a mitotic arrest. Bottom, quantification of Cdc20 isoform levels. The levels in the undiluted HeLa sample (50 μg) were set to 1. (**B**) Western blot as in (A) showing synchronized U2OS cells harvested at different times post-release. The ratio of full-length:M43 isoforms was quantified at the indicated time points. (**C**) Western blot of immunoprecipitated APC/C to detect the APC/C and bound Cdc20 from single-thymidine synchronized U2OS cells post-release into medium with STLC for 15 hrs (short mitotic arrest) or 22 hrs (long mitotic arrest). (**D**) Top, Western blot showing mitotically-arrested U2OS cells harvested at indicated time points after cycloheximide addition to inhibit new protein synthesis. Bottom left, graph of average Cdc20 protein levels quantified from two experimental replicates with levels in untreated cells set at 100%. Bottom right, representative phase contrast images of cells at 3 hrs post-cycloheximide addition or corresponding untreated cells. Scale bar, 50 μm. (**E**) Western blot showing mitotically-enriched HeLa or U2OS cells after 2 hr treatment with either cycloheximide or the proteasome inhibitor MG-132. Bottom, quantification of Cdc20 isoform levels with levels in untreated cells set to 1.

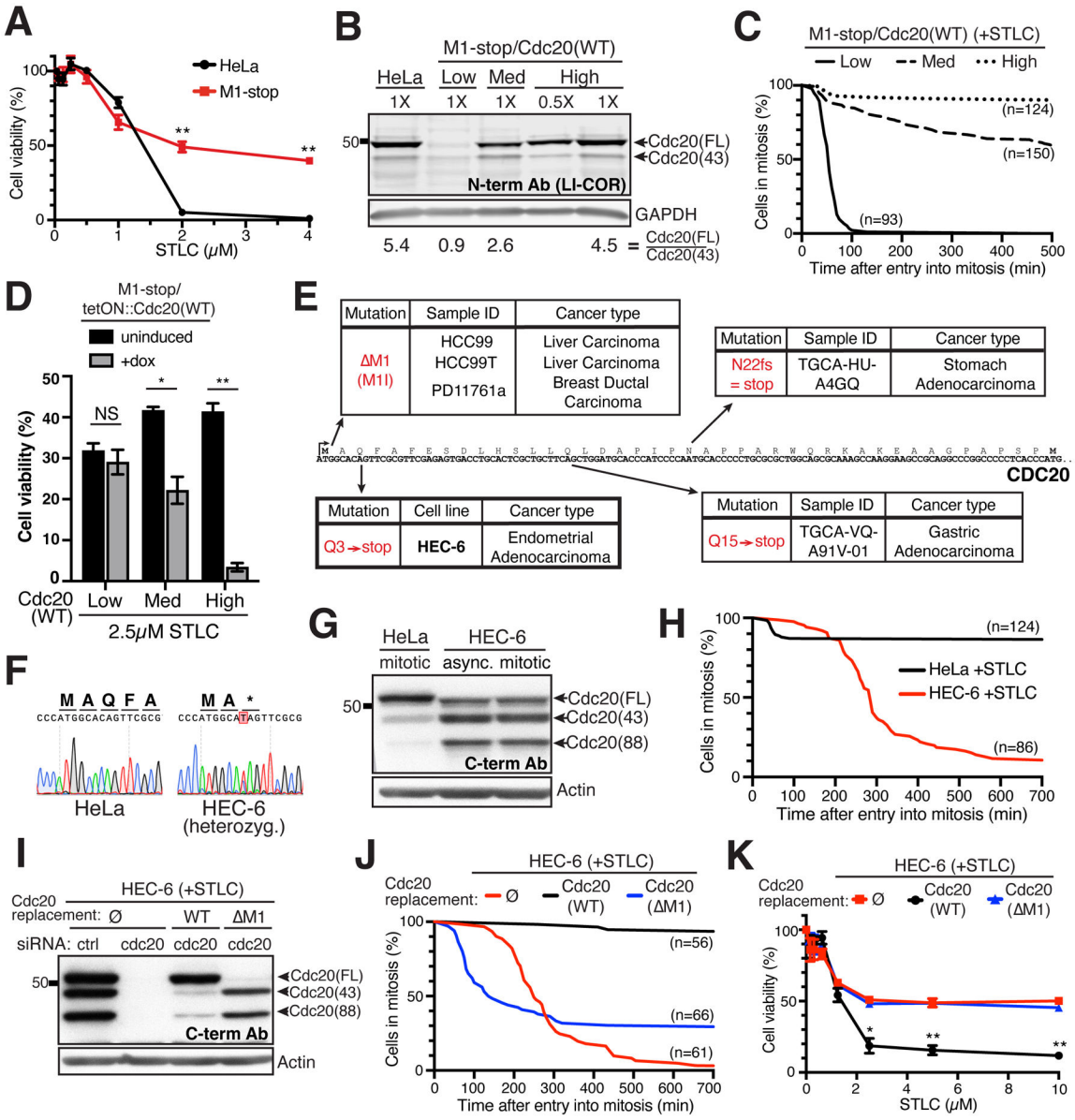

Figure 5. Cdc20 proteoform levels alter anti-mitotic drug sensitivity.

(**A**) Sensitivity of HeLa or M1-stop cells to increasing STLC concentrations by MTT viability assay. (**B**) Western blot of mitotically-enriched HeLa or M1-stop mutant with low, medium, or high expression of doxycycline-inducible *CDC20(WT)* construct induced with 20 ng/ml doxycycline. Numbers are the average ratio of full-length:M43 isoforms from three experimental replicates. (**C**) Cumulative frequency distribution for the fraction of cells in mitosis at the indicated time after mitotic entry (mitotic arrest duration) for the representative clones in (B) treated with STLC. The total number of cells analyzed across two experimental replicates is indicated. (**D**) Cell viability (MTT assay) after treatment with 2.5 μM STLC for the representative clones in (B-C) with or without doxycycline induction. (**E**) Tumors and cancer cell lines from public databases with *CDC20* mutations that are predicted to selectively alter the full-length protein. (**F**) Sanger sequencing of

CDC20 gene in HEC-6 cell line with the M1 start codon region highlighted. (**G**) Western blot comparing HeLa and HEC-6 using antibodies recognizing Cdc20 C-terminus. (**H**) Cumulative frequency distribution as in (C) for HeLa and HEC-6 cells treated with STLC. (**I**) Western blot as in (G) for HEC-6 cells expressing mEGFP alone or the indicated *CDC20* construct treated with either control or Cdc20 siRNAs. (**J**) Cumulative frequency distribution as in (C) for HEC-6 cells either expressing mEGFP treated with control siRNAs or with endogenous Cdc20 protein replaced with the indicated *CDC20* construct. (**K**) STLC drug sensitivity as in (A) for HEC-6 cells either expressing mEGFP treated with control siRNAs or with endogenous Cdc20 protein replaced with the indicated *CDC20* construct. Data in (A,D,K) are mean ± s.e.m from three experimental replicates, Student's two-sample t-Test with two-tailed distribution comparing cell viabilities per drug concentration (*$p < 0.05$, **$p < 0.01$).

Extended Data Table 1.

The SAC is defective in ΔM1 and M1-stop mutant cell lines. Related to Extended Data Figure 4.

Mitotic arrest duration in the presence of 10 μM STLC for control HeLa compared to the ΔM1 and M1-stop mutant cell lines with the indicated drug or RNAi treatment (see Extended Fig. 4F-G). Indicated is the mean mitotic duration ± standard deviation across two experimental replicates. The total number of cells analyzed is provided in brackets. Statistics from Mann-Whitney Test (****p < 0.0001, NS not significant).

	Mitotic time (min)		
	HeLa	**ΔM1**	**M1-stop**
STLC/DMSO	780±203 (n=103)	60±24 (n=97)	67±12 (n=85)
STLC/Mps1i (4μM)	43±37 (n=89)	56±19 (n=79)	60±13 (n=98)
	<0.0001 (****)	NS	<0.001 (***)
STLC/siCtrl	805±168 (n=122)	65±37 (n=88)	70±18 (n=90)
STLC/siMad2 (24hr)	284±225 (n=106)	57±25 (n=99)	59±20 (n=97)
	<0.0001 (****)	NS	<0.0001 (****)